Development of hyaluronic acid – poly(ethylene glycol) hydrogels towards hematopoietic differentiation of mouse embryonic stem cells

by

Kathryn Marie Erickson, B.S.

Thesis

Presented to the Faculty of the Graduate School of

The University of Texas at Austin

in Partial Fulfillment

of the Requirements

for the Degree of

Master of Science in Engineering

The University of Texas at Austin

August 2009

The Thesis committee for Kathryn Marie Erickson

Certifies that this is the approved version of the following thesis:

Development of hyaluronic acid – poly(ethylene glycol) hydrogels towards hematopoietic differentiation of mouse embryonic stem cells

APPROVED BY

SUPERVISING COMMITTEE:

Supervisor: ______________________________

Krishnendu Roy

____

Laura Suggs

Dedication

To my parents, Carolyn and Edward Erickson, for listening to all my long phone calls home and providing me with constant love, advice, support, and encouraging me to follow my heart and make the best choices for my life. Mommy and Daddy, you have always been my parents but, I love that I can say you are my best friends.

To my brother, Jeffrey Erickson, who introduced the field of Biomedical Engineering to me and was ever-willing to impart his knowledge over the phone throughout my undergraduate and graduate years. Thank you for being my teacher and more importantly thank you for being my friend.

To my grandparents, Nana, Pop-pop, Grandma, and Grandpa, who all passed before they could see me grow into the person I am today. I know you are all watching over me and guiding me in every step I have and will take in life. I can only hope that I have made you proud.

To my Austin Wildcats family who gave me the opportunity to do what I love and make a difference. Thank you for being my Texas family and helping me to find myself again.

"Seeker there is no path. The path is made by walking."

The path in life you choose may not make sense to others, but you must choose the path which will fulfill you as a person. Be unafraid of change. Take chances. And just LIVE.

Acknowledgements

I would like to thank all of the members of The Laboratory for Cellular and Macromolecular Engineering who have helped me develop into a researcher. First, I want to thank Dr. Krishnendu Roy for being my advisor and teacher for the past three years. I feel fortunate to have been mentored by an enthusiastic researcher but more importantly, I was lucky to have such a genuinely good person as my PI for three years. Thank you to Dr. Laura Suggs for agreeing to be the second reader on this thesis. I would also like to thank all of my co-workers who shared their knowledge and taught me valuable skills throughout my time at the University of Texas at Austin especially, Ankur, Mary, Julie, Zach, and Irina.

Thank you to all of my family and friends who were a constant support system. Thank you for listening. Thank you for making me laugh *loudly*. Thank you for making me smile. After all, people are what make experiences worth while. Lastly, and most importantly, I need to thank God who is the ultimate voice of reason and the greatest compass in my life.

Abstract

Development of hyaluronic acid – poly(ethylene glycol) hydrogels towards hematopoietic differentiation of mouse embryonic stem cells

Kathryn Marie Erickson, M.S.E.

The University of Texas at Austin, 2009

Supervisor: Krishnendu Roy

The fields of tissue engineering, regenerative medicine, and stem cell engineering are rapidly growing. However, these fields must overcome several obstacles before they can make a significant impact on treating cellular disorders. Two major hurdles that must be addressed are: determining how to control the pluripotency of stem cells and developing systems for high-throughput culture of stem cells. The prospect of using a cell source capable of differentiating into cells of any tissue in the body (embryonic stem cells) has received enormous interest in

recent years. The pluripotent attribute of embryonic stem cells seems ideal but developing methods to drive embryonic stem cells to specific lineages, including the hematopoietic lineage, is a complex process dependent on multiple intrinsic and extrinsic factors including chemical, cellular, and environmental signaling. With regards to environmental signaling, the use of three-dimensional culture systems such as scaffolds and hydrogels, have been utilized in an attempt to drive lineage-specific differentiation in a synthetic, biomimetic microenvironment. To determine specific environmental factors responsible for hematopoietic differentiation a systematic biological and engineering process must be implemented.

A biodegradable hydrogel composed of the hyaluronic acid, a polysaccharide abundant in the bone marrow microenvironment, and the synthetic polymer, poly(ethylene glycol) was formulated to culture mouse embryonic stem cells (mESCs). Photoencapsulation of mESCs did not significantly decrease cellular viability or proliferation. The FACS data was inconclusive however, from gene expression studies, it was determined that the hydrogel culture system promoted differentiation of mESCs as evidenced by a down-regulation of the gene encoding for stem cell maintenance transcription factor, Oct-3/4. Furthermore, embryoid bodies, necessary for *in vitro* differentiation were observed in the hydrogel systems. Although an increase in the gene encoding for the cell surface marker, c-kit was up-regulated, the surface marker, sca-1 was not up-regulated. Up-regulation of both c-kit and sca-1 is necessary for the development of hematopoietic progenitor cells.

Results indicate that the differentiation of mESCs into the hematopoietic lineage was unsuccessful but differentiation in these hydrogel systems did occur. Future cell marker and gene expression studies are necessary to determine which cell lineage the encapsulated mESCs are differentiating into before the effects of incorporating other environmental, cellular, and chemical factors can be investigated.

Table of Contents

List of Tables

List of Figures

Chapter 1: Introduction

The prospect of treating a wide variety of cellular disorders with cell replacement therapy is becoming ever more realistic. For this reason, cellular therapeutic research is becoming increasingly popular. However, the field is currently limited by the number of donor cell sources. The future success of cell therapy in disease treatment is strongly dependent on the development of a widely available donor source. Due to their pluripotent and self-renewing nature, stem cells are an extremely attractive source for cell therapy. The creation of a high-throughput culture system capable of driving the differentiation process of stem cells is critical for the ultimate clinical success of cellular therapeutics.

Currently, hematopoietic stem cells (HSCs) are used in cell replacement therapies to treat blood disorders such as leukemia, lymphoma, and myeloma. HSCs used in cell therapy are isolated from the bone marrow of a donor or the patient and then transplanted into the patient [1]. Limitations to HSC transplantation include a lack of efficient methods for both HSC extraction from the bone marrow and *in vitro* expansion of HSCs as well as a scarcity of matching donors [1]. If an "off-the-shelf" HSC supply were available, difficulty in both HSC extraction and the location of suitable donors would be eliminated. However, the problem of developing of a high-throughput *in vitro* system specific to HSC expansion still remains. To solve this problem, a basic understanding of HSC development and biology must be obtained.

It is well known that three-dimensional (3D) cultures enhance cell-cell and cell-environment interactions and further mimics the *in vivo* environment. Mouse embryonic stem cells (mESCs) cultured on tantalum-based scaffolds and poly(L-lactic acid) (PLLA) - based scaffolds have been shown to increase the efficiency of hematopoiesis [2, 3]. Other studies have shown hyaluronic acid (HA) hydrogels promote embryonic stem cell proliferation [4]. The next natural step is to direct stem cells to differentiate into one specific cell line: the hematopoietic lineage. We proposed to take a systematic biological approach to mimic the bone marrow microenvironment cellularly, molecularly, and environmentally. A combination of a biocompatible material with specific niche proteins may enhance hematopoietic differentiation of mESCs in a controlled and repeatable manner.

Chapter 2: Background

2.1 Embryonic stem cells and hematopoiesis

Stem cells (SCs) are an invaluable self-renewing cell population present throughout the human body. In times of severe stress when an organ needs repair, SCs specific to an organ are able to replenish the cell population. Embryonic stem cells (ESCs), first isolated in 1981 from the inner cell mass of a murine blastocyst , are able to perpetually proliferate in an undifferentiated state and differentiate into multiple cell lineages [5]. In an effort to maintain homeostasis, SCs constantly make a choice to either self-renew or differentiate [6, 7]. This decision is a result of both intrinsic, cellular and extrinsic, microenvironmental factors [6, 7]. Their pluripotent attribute makes ESCs an extremely attractive cell source for tissue engineering and regenerative medicine applications. To date, researchers have been able to promote differentiation of ESCs into several cell lineages including vascular, neural, hepatic, chondrogenic, pancreatic, and osteogenic lineages [8-14]. In recent years, studies have emphasized hematopoietic differentiation given the widespread clinical applicability of hematopoietic stem cells (HSCs) [3].

Hematopoiesis is the development of blood cellular components including erythrocytes, granulocytes, and lymphocytes. The initial location of hematopoiesis is the yolk sac in an embryo, specifically in the blood islands [3, 7, 15, 16]. This occurs around day 7.5 of gestation [7, 16]. As development progresses, the site of hematopoiesis relocates around day 10 of gestation to the aorta-gonadmesenephros and then to the placenta [13]. From day 12 of gestation until birth, hematopoiesis occurs in the fetal liver and spleen [13, 7, 16]. Hematopoiesis reaches its final destination at birth in the bone marrow [7, 15, 16].

HSCs and hematopoietic progenitor or precursor cells (HPCs) ultimately give rise to blood components [15]. Current *in vitro* methods of differentiating stem cells involve the formation of embryoid bodies (EBs) in suspension culture [17]. These ball-like structures physically resemble the embryo in its initial developmental stages [18]. More applicable to stem cell differentiation research is the cellular composition of EBs. EBs contain cells which delineate the three germ layers: ectoderm, mesoderm, and endoderm [16]. Between day 2.5 and day 4 of EB culture, multiple precursor cell types, including HPCs, capable of differentiating into a variety of cell lineages develop [7, 19]. The germ layer of interest in HSC research is the mesoderm because HPCs along with endothelial, cardiac, skeletal, and adipocyte precursors are located here throughout development [16]. Although EBs contain the germ layer and cell lineage of interest, a major obstacle in HSC research is the development of an effective, high-throughput hematopoietic *ex vivo* system. HSCs cultured *in vitro* and implanted have been shown to have a decrease in engrafting and self-renewal capabilities [7]. Therefore an *in vitro* system combining hematopoietic chemical and physical stimuli with EB production could be directed to yield large-scale supplies of HPCs and HSCs. In the future, HSC supplies can be used in the treatment of blood disorders including anemia, lymphoma, leukemia, and myeloma.

Although efforts to create a high-throughput system for the generation of HSCs have improved with an increased use of 3D and dynamic culture systems, the biological effects of the microenvironmental factors on the hematopoietic differentiation process has not been studied in depth. In order to make strides in optimizing a high-throughput HSC differentiation culture system, the environmental effects on the differentiation process must be examined. This study investigated the genetic and molecular effects on mESCs when cultured in a fabricated bone marrow microenvironment.

2.2 The bone marrow and the stem cell niche

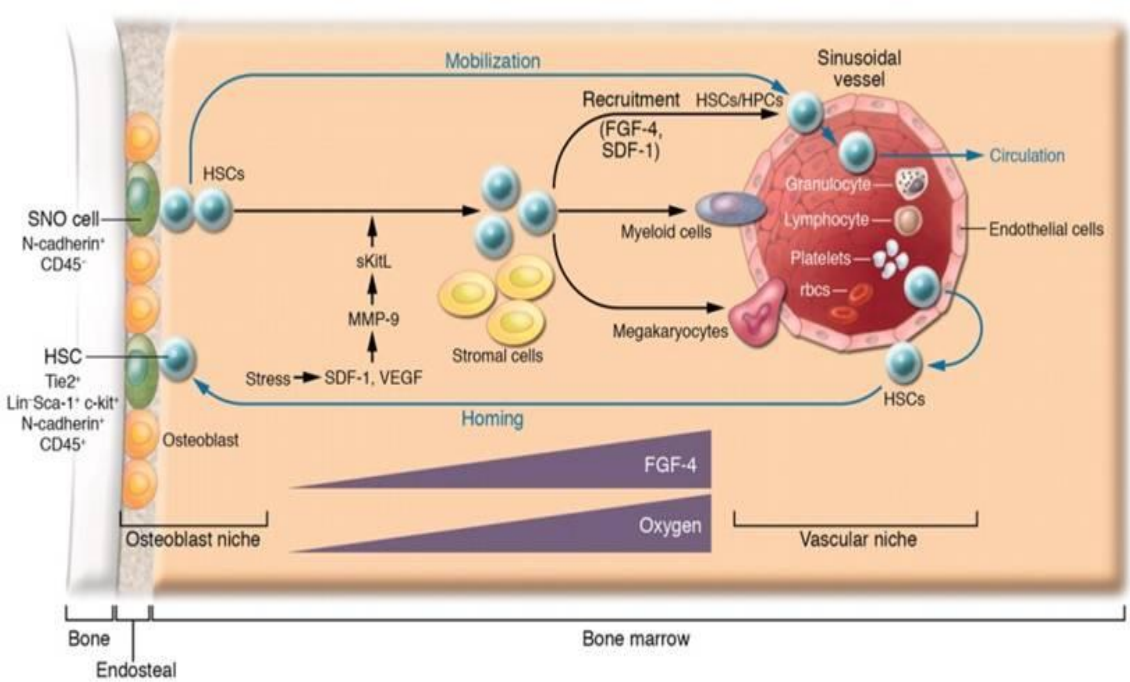

Figure 2- 1. The bone marrow HSC niches. from Yin *et. al.*. *The stem cell niches in bone*. Journal of Clinical Investigation 116:1195-1201, 2006.

The bone marrow is a soft anatomical structure situated in the bone cavity [15]. It houses specialized microenvironments, known as stem cell "niches," vital to stem cell functions [15, 20]. Niches consist of specific extracellular matrices (ECM) and supporting cell lines which cooperatively function to control the major stem cell operations: self-renewal, quiescence, and differentiation [15, 21]. The bone marrow is known to have two HSC niches which manage hematopoiesis: the endosteal or osteoblastic niche and the vascular niche [15, 20]. The endosteal niche, classified as a quiescent environment, houses "slow-cycling" long-term HSCs responsible for the maintenance of the HSC supply or pool [20]. HSC proliferation and differentiation occurs in the vascular niche, where "actively-cycling" short-term HSCs supply the body with circulating HSCs and HPCs [15, 20].

Supporting evidence from immunofluorescent transplantation studies tracked transplanted HSCs in mice to their final location in the bone marrow. Results showed cells which had not committed to a lineage (Lin $^{-}$ cells) migrated to the endosteum of the bone [22]. Lin $^{+}$ cells, or cells with a determined lineage, migrated to the central region of the bone marrow [22]. These results lead to the hypothesis of the endosteal niche being the more important of the two HSC niches. Although the vascular niche sources the body with blood cells, the endosteal niche is the supplier of HSCs to the vascular niche. Without the endosteal niche, a life-time continuance of hematopoiesis is not possible [20].

2.3 Three-dimensional stem cell culture

The goal of a tissue engineering culture system is to mimic the *in vivo* environment of the tissue. Extensive tissue engineering research has been performed using two-dimensional (2D) culture systems; however, the body is three-dimensional. Furthermore, the body and its organ systems are not static but are dynamic. Circulation of nutrients, hormones, oxygen, and carbon dioxide through the vascular system introduces fluid flow into tissue microenvironments. For these reasons, 2D culture systems are not indicative of the natural cellular environment and therefore tissue engineers have begun to implement 3D and dynamic culture systems.

Recent studies have demonstrated the effective differentiation of embryonic stem cells (ESCs) in 3D biomaterials [2-4, 10, 23]. The utilization of biomaterials to create 3D cellular environments in the form of scaffolds and hydrogels has become increasingly prevalent in stem cell research. Scaffolds and hydrogels, essentially serve as an artificial ECM leading to successful differentiation studies. With their controllable porosity, scaffolds create a cellular environment conducive to nutrient flow, matrix construction, cell-matrix, and cell-cell interactions [18]. mESCs cultured in scaffolds constructed with fibrin have been shown to differentiate into the vascular lineage [10]. PLLA scaffolds and tantalum-based scaffolds have been employed in hematopoietic differentiation of mESCs [3]. Moreover, the addition of dynamic nutrient flow (i.e. spinner flask cultures) has increased hematopoietic differentiation efficiency [2].

Studies have also revealed the potential use of hydrogels as biomimetic culture systems for proliferation and guided differentiation of human embryonic stem cells (hESCs) [4]. Hwang *et al.* have proven successful guided chondrogenic differentiation of mESCs in poly(ethylene-glycol) (PEG) hydrogels in combination with a growth-factor enhanced culture medium [23]. Their most recent undertaking involves the actual incorporation of ECM constituents within their PEG-based hydrogel; however, this study was performed with primary chondrocytes not ESCs [24]. ECM hydrogels have yet to be investigated in hematopoetic differentiation of ESCs.

2.4 HSC-niche interactions

The "cross-talk" between HSCs and the endosteal niche is essential for transmitting the proper molecular signals involved in hematopoiesis [21]. The ECM and specialized cells within the niche are thought to communicate with the stem cells through cell-cell and cell-matrix interactions which have not been studied in detail [20, 21]. The role of the endosteal niche ECM is not characterized in detail but key ECM components including fibronectin, collagen type I, and collagen type IV have been identified through immunohistochemical staining [25]. A more recent study identified the glycosaminoglycan, hyaluronic acid (HA), as another key ECM component. HA is the third main glycosaminoglycan, in terms of quantity, generated by the supporting, stromal cells in the bone marrow [22]. HA composes approximately 40% of glycosaminoglycans generated by the stromal cells. [22, 26] It functions in the suppression of HSC proliferation and differentiation as well as HSC lodgement within niches [21, 22]. Physical contact with ECM components in a biomimetic microenvironment may trigger differentiation and signal transduction pathways associated with hematopoiesis.

2.5 Hyaluronic Acid

First discovered in the vitreous humor of the eye by Karl Meyer in 1934, HA is a linear, high molecular weight, negatively charged, and acidic glycosaminoglycan composed of two repeat units: D-glucaronic acid β-1 and 3-N-acetylglucosamine-β-1,4 [27-29]. Naturally occurring HA has a molecular weight ranging from 10^5 – 10^7 Daltons and the most common sources of HA for experimental use include the umbilical cord, rooster comb, joint fluids, and streptococci [27-29]. Studies done by Scott *et al.* in 1989 revealed the secondary structure of HA to be helical in nature with hydrogen bonds joining the linear polymer chains together [30]. The presence of hydrogen bonds allows for the polymer to easily interact with water, creating an expanded, coiled structure with a large hydrodynamic radius (20 nm) and high viscosity [28, 29]. These structural properties make HA an ideal polymer distributed throughout the body's ECM for lubrication, space-filling, and load-bearing functions [28]; however, HA also has key roles in the body's molecular interactions.

2.6 The role of hyaluronic acid in the bone marrow

As previously stated, HA is a key component of the bone marrow ECM and the HSC niche [21, 22, 27]. Studies have reported the importance of HA in a number of cellular functions including tissue repair, cell migration, cell proliferation, and most importantly cell differentiation [27, 31]. Through its interactions with hyaladherins (HA binding proteins) including aggrecan and link proteins, HA imparts structural integrity on the bone marrow microenvironment and helps to contain HSCs within the marrow [27, 28]. It also participates in receptor-ligand interactions primarily through the cell surface receptor, CD44H (CD44, hematopoietic) leading to activation of intracellular signaling cascades [28, 32-35]. About 50% of total GAG synthesis in the bone marrow is a result of HA synthesis by supporting/stromal cells as well as the sinusoidal endothelium of the vascular niche and cells on the endosteal surface [26, 36]. The polymer is also synthesized by hematopoietic progenitor cells (HPCs), specifically $Lin^{-}Sca^{+}Kit^{+}$ HPCs [22]. Given the presence of HA in the HSC niche (i.e. the endosteal niche) and the production of HA by hematopoietic stem cells, the introduction of HA in an artificial, biomimetic microenvironment may lead to differentiation of mESCs into the hematopoietic lineage.

Chapter 3: Materials and Methods

3.1. Hydrogel synthesis and characterization

3.1.1 Methacrylation of Hyaluronic Acid

Methacrylated HA was synthesized according to a protocol from Leach *et. al.* [37]. Briefly, 0.5 grams of HA (Sigma-Aldrich, St. Louis, MO) was mixed with 50 milliliters of a 50:50 dH_2O: acetone (Fisher Scientific) solution overnight to allow for full dissolution. 3.6 milliliters of triethylamine (Sigma Aldrich, St. Louis, MO) was added to the solution and allowed to stir in a closed container for approximately 2 hours after which, 3.6 milliliters of glycidyl methacrylate (Sigma Aldrich, St. Louis, MO) was added and allowed to stir in a closed container in the dark for 24 hours. To collect a solid, purified methacrylated HA (MeHA) product two reprecipitations of MeHA in acetone (1:20) were conducted. Following each reprecipitation, the solid product was redissolved in 50 milliliters of dH_2O overnight. After the second reprecipitation and dissolution, 8 milliliter aliquots of the solution were transferred to 15 milliliter centrifuge tubes. The aliquots were frozen at -20^{0}C for approximately 2 hours and then transferred to -80^{0}C for overnight and long-term storage. The frozen aliquots were lyophilized for 3 days to obtain a solid product of methacrylated HA. NMR was performed on freeze-dried samples to verify methacrylation.

3.1.2 HA hydrogel and HA-PEGDA "co-gel" formation

Poly(ethylene glycol) diacrylate (PEGDA) (MW 3400, Laysan Bio, Arab, AL) and HA "co-gels" as well as pure HA hydrogels were generated similar to methods used by Gerecht *et. al.* [4]. Briefly, PEGDA was dissolved in Phosphate Buffered Saline (PBS) at two concentrations (2% and 3% w/v); three concentrations of HA were utilized (1%, 1.5%, and 2% w/v). HA was added to the PEGDA-PBS solution and allowed to rotate overnight at room temperature allowing for complete dissolution. 0.05% (w/v) of the photoinitiator, Irgacure 2959, was mixed into the solution. 100 μl of the polymer solution was pipetted into separate wells of a 96-well tissue culture plate and placed under a UV lamp (Mercury Spot Lamp, Ted Pella Inc., Redding, CA) at an intensity of ~7.5 mW/cm^2 until gelation occurred after approximately 9 to 10 minutes. Fully cured hydrogels were then transferred to separate wells of a 24-well tissue culture plate and covered with 1 milliliter of PBS.

3.1.3 Determining degradable HA-PEGDA hydrogels

To ensure complete degradation and cell release from HA-PEGDA co-gels, studies were performed using bovine hyaluronidase (Sigma-Aldrich, St. Louis, MO). Following the protocol from Gerecht *et. al.* [4], hyaluronidase was added to each hydrogel sample at varying concentrations (500 U/ml, 1,000 U/ml, 1,500 U/ml, 2,000 U/ml) and incubated for 24 hours at 37^0C on a rotator. After 24 hours, samples were pipetted out and inspected for any solid hydrogel remnants. Co-gels incapable of full degradation were not used in any further studies.

3.1.4 Degradation Studies

Degradation profiles were created by modifying a protocol by Leach *et. al.* [38]. The following hydrogels were formed as described above: 1%HA, 1.5%HA, 2.0%HA, 1%HA-2%PEGDA, 1.5%HA-2%PEGDA, 1%HA-3%PEGDA, and 1.5%HA-3%PEGDA. Each hydrogel was blotted dry with a kimwipe and weighed on a microscale prior to enzymatic treatment. All gels were transferred to separate wells of a 24-well tissue culture plate and 1 milliliter of a 2,000 U/ml hyaluronidase (Sigma-Aldrich, St. Louis, MO) solution was added to each gel. At each time point hydrogels were transferred to positively charged microscope slides and carefully blotted with a kimwipe before measuring the remaining mass. Time points for pure HA hydrogels were taken every 15 minutes until full degradation of the hydrogel network occurred. Time points for HA-PEGDA co-gels were taken every hour until full degradation was observed.

3.1.5 Swelling Studies

A protocol used by Tan *et. al.* was modified to obtain swelling ratios (Q) of degradable hydrogels [39]. The following hydrogels were formulated as described above: 1%HA, 1.5%HA, 2%HA, 1%HA-2%PEGDA, 1.5%HA-2%PEGDA, 1%HA-3%PEGDA, and 1.5%HA-3%PEGDA. Hydrogels were allowed to swell in 1 milliliter of PBS at 37^0C for 72 hours. PBS was changed after the first 24 hours to remove excess polymer remnants. Swollen hydrogels were carefully blotted on a kimwipe and swollen weights (M_s) were obtained with a microscale. These hydrogels were then transferred to 1.5 milliliter microcentrifuge tubes and frozen at -20^0C for ~2 hours followed by a freezing at -80^{0}C overnight. Using a 22 gauge needle tip, a hole was made in the caps of the centrifuge tubes and samples were freeze-dried for ~24 hours. Dry weights (M_d) were then obtained by carefully weighing lyophilized hydrogels with a microscale. The mass-based swelling ratio was defined as $Q = \frac{Ms}{Md}$ [40].

3.1.6 Compressive Modulus

Hydrogels and co-gels were formulated, as described above, and allowed to swell in PBS for 72 hours. The compressive modulus of hydrogels was measured using Instron® In-Spec 2200 benchtop apparatus and a Sony CLIÉ® Handheld device. Gels were compressed at a rate of 0.001mm/second. Load and compression values were recorded in the Sony CLIÉ® Handheld device and then transferred into text and Excel files. Stress was calculated using the following equation: $\sigma = \frac{F}{A}$, where F is the force in Newtons and A is the area of the hydrogel. Strain was calculated with the following equation: $\varepsilon = \frac{\Delta l}{lo}$, where Δl is the recorded compression (mm) and l_o is the initial height (mm) of the hydrogel. The compressive modulus was determined by plotting stress versus strain and determining the slope of the first linear portion of the graph.

3.2. Mouse embryonic stem cell culture and expansion

3.2.1 Feeder layer culture and inactivation

The use of a feeder layer or leukemia inhibitory factor (LIF) is necessary to maintain stem cells in an undifferentiated state [41]. Initially a feeder layer of mouse embryonic fibroblasts, STO (Sandoz inbred mouse thiguanine-resistant ouabain-resistant) cells, were irradiated and utilized. The feeder layer was then changed to another mouse embryonic fibroblast line, MEFs. 5 x10^5 MEF cells were seeded on two gelatin-coated T-25 tissue culture flasks. Media was changed every 2-3 days and MEFs were allowed to grow to ~80% confluency before inactivation with mitomycin C or passaging. One T-25 flask of confluent MEFs was inactivated with a 10 μg/ml mytomycin C solution in DMEM with 5% embryonic stem cell screened defined Fetal Bovine Serum (ES-screened FBS) (StemCell Technologies, Vancouver, BC, CA), for approximately 3 hours at 37^0C. After 3 hours, cells were rinsed with sterile PBS and replaced with MEF growth medium. The second T-25 flask of MEFs was passaged at a ratio of 1:6 onto two gelatin-coated T-75 tissue culture flasks. After these flasks reached confluency, they were inactivated with mytomycin C as previously described. Inactivated flasks were utilized during mESC expansion.

3.2.2 Expansion of undifferentiated R1 mESCs

The mESC cell line, R1, (A. Nagy, Mount Sinai Hospital, Ontario, Canada) was cultured with similar methods described by Taqvi *et. al.* [3]. mESCs were cultivated on a feeder layer of mitomycin C inactivated MEFs (I-MEFs) in R1/MEF medium consisting of complete DMEM medium (Hyclone, Logan, UT) with 20% defined ES-screened FBS (StemCell Technologies, Vancouver, BC, CA), 2mM L-glutamine, 1mM sodium pyruvate, 0.1mM non-essential amino acids, 5 x10^{-5} 2-mercaptoethanol (Invitrogen, Carlsbad, CA), 100 U/ml penicillin G (Hyclone, Logan, UT), and 10 μg/ml streptomycin (Hyclone, Logan, UT). The addition of 1,000 U/ml LIF maintains the R1 cells in an undifferentiated state. 5×10^5 – 1×10^6 R1 cells were seeded on a T-25 flask of I-MEFs and allowed to culture for two days at 37°C, 5% CO_2 with daily medium changes. After 2 days, R1 cells were passaged at a 1:6 ratio onto two T-75 flasks of I-MEFs and allowed to culture for two more days before proceeding to the pre-differentiation step.

3.2.3 Pre-differentiation of R1 mESCs

The first step of pre-differentiation is the removal of feeder cells from expanded R1 mESCs. R1 cells cultured on top of I-MEFs were trypsinized for ~2 minutes at 37°C and pelleted at 4°C for 5 minutes at 300 x g. Pellets were resuspended in R1 expansion medium and replated in 10 milliliters R1/MEF medium onto two T-75 tissue culture flasks without gelatin coating. Flasks were allowed to incubate at 37°C, 5% CO_2 for 10 minutes to allow feeder cells to adhere to the flask. The medium was removed from each flask and non-adherent cells were pelleted as previously stated. Cell numbers were obtained using a hemocytometer. R1 cells were then seeded onto gelatin-coated T-150 tissue culture flasks at a density of 1×10^6 cells per flask. R1 cells were cultured for two days in R1 pre-differentiation medium consisting of complete IMDM medium (Hyclone, Logan, UT), 15% defined ES-screened FBS (StemCell Technologies, Vancouver, BC, CA), 0.1mM non-essential amino acids, 5×10^{-5} 2-mercaptoethanol (Invitrogen, Carlsbad, CA), 100 U/ml penicillin G, and 10 μg/ml streptomycin. Medium was supplemented with

1,000 U/ml of LIF. After two days, R1 pre-differentiated cells were trypsinized for ~2 minutes at 37^{0}C, 5% CO_2 and collected for use in differentiation experiments.

3.3 Mouse embryonic stem cell differentiation

3.3.1 Embryoid body formation

To promote EB formation, a modified version of the protocol used by Liu *et. al.* was followed to create two-dimensional (2D) controls. R1 cells were seeded on 100 mm bacteriological plastic plates at a density of 1 x 10^5 cells per milliliter. Cells were cultured in 10 milliliters of R1 differentiation medium used by Liu *et. al.* containing complete IMDM medium (Hyclone, Logan, UT), 15% ES-Cult FBS (Stem Cell Technologies, Vancouver, BC, Canada), 2mM L-glutamine, 100 U/ml penicillin G, 10 µg/ml streptomycin, 0.1mM non-essential amino acids, and 5x10^{-5} 2-mercaptoethanol. To promote differentiation, the medium was not supplemented with LIF. Medium was changed every 3 to 4 days by pipetting out all 10 milliliters of the EB-media solution into 15 milliliter centrifuge tubes. These tubes were closed and left open by quarter turn before placing them at 37^{0}C, 5% CO_2 for approximately 30 minutes to allow the EBs to fall. After gravitational pelleting, 5 milliliters of medium was removed from the top of the pellet and replaced with a fresh 5 milliliters of medium. The pellet was resuspended with gentle pipetting and returned to the 100 mm bacteriological plate for further culture.

3.3.2 mESC encapsulation

As previously stated, an essential step in *in vitro* differentiation is the formation of EBs. In a hydrogel culture system, EBs can be formed after seeding stem cells inside the gel. R1 expansion and pre-differentiation was followed by photoencapsulation, as described above, at a concentration of approximately 1 x 10^6 cells per hydrogel. After gelation occurred, the resulting hydrogels were removed from the sterile, 96-well tissue culture plates and transferred to individual wells of a 24 –well tissue culture plate. 1 milliliter of R1 differentiation medium was added to each well. Samples were then incubated at 37^0C, 5% CO_2 for two to three hours after which medium was changed to remove any hydrogel and photoinitiator remnants which may have leached out. mESC encapsulated hydrogels were cultured for various time points including days 3, 7, and 10 depending on the assay being performed.

3.4. Microscopy Imaging

3.4.1 Cell fixation in hydrogels

Cells and EBs were fixed in hydrogels to allow for both DAPI staining and scanning electron microscopy. Hydrogels were transferred to separate wells of a 24-well tissue culture plate and underwent three series of five minute PBS rinses. 1 milliliter of a 4% paraformaldehyde solution was added to each gel. The gels were incubated on ice in the fixative for 15 minutes followed by either DAPI staining or another three series of five minute PBS rinses. Fixed gels were stored at 4^0C.

3.4.2 DAPI staining

Encapsulated R1 cells in 1.5%HA – 3%PEGDA gels were fixed as described above. Using a modified version of the protocol from the manufacturer (Molecular Probes), encapsulated cells were stained on ice with ~600 µl of a 14.3 mM stock solution of DAPI dihydrochloride for 10 minutes. Hydrogels then underwent three, 5 minute PBS rinses to remove any excess staining. Hydrogels were stored at 4^0C until sample preparation for confocal microscopy. Silicon spacers (Invitrogen, Carlsbad, CA) were stacked on a microscope slide to create a chamber for each hydrogel. Hydrogels were placed in the circular chambers of the spacers and one drop of Vectashield mounting medium for fluorescence (Vector Laboratories, Inc., Burlingame, CA) was added to each chamber to eliminate any background signal. A cover slip was carefully placed on top of the samples to avoid any air bubble formation and clear nail polish was used to seal the cover slip. The Core facility's confocal microscope (University of Texas Core facility) was used to obtain fluorescent and Normalsky images of EBs and cells encapsulated in 1.5%HA – 3% PEGDA hydrogels.

3.4.3 Scanning electron microscopy

Cells and EBs encapsulated in the hydrogels were fixed as described above. Hydrogels were dehydrated using a series of ethanol washes. The following ethanol dilutions were used: 30%, 50%, 60%, 70%, 80%, 90%, and 100%. Hydrogels were transferred to separate wells of a 12-well tissue culture plate. 1 milliliter of 30% ethanol was added to each well and was incubated at room temperature for 30 minutes. The ethanol was then removed and 50% ethanol was added. The same procedure was followed for all subsequent dilutions of ethanol. After the hydrogels were fully dehydrated, they were mounted on SEM stubs and stored in a dessicator until sputter coating and imaging. Mounted and dried hydrogels were sputter coated with Platinum-Palladium or Iridium using the sputter coater at the Core facility (University of Texas Core facility). SEM images were obtained with the Core facility's instrument, Zeiss Supra 40 VP .

3.5. Cell viability and proliferation

3.5.1 Propidium Iodide staining

To assess cell viability of encapsulated R1 cells, a propidum iodide (PI) stain was performed on Day 3. Cells were collected, washed twice with 1 milliliter of FACS buffer, and resuspended in FACS buffer as described below in section C.6.2. 3 μl of PI was added to each sample immediately before performing flow cytometry using the Core facility's (University of Texas Core Facility) FACS Calibur. MEF cells were used as a positive control.

3.5.2 Cell proliferation assays

To assess cell proliferation, the CellTiter 96® AQ_{ueous} One Solution Cell Proliferation Assay kit (Promega) was utilized as well as a Carboxyfluorescein diacetate, succinimidyl ester (CFSE) assay (Molecular Probes). Hydrogels and 2D cultures were stained with a tetrazolium compound [3-(4,5-dimethylthiazol-2-yl)-5-(3-carboxymethoxyphenyl)-2-(4-sulfophenyl)-2H-tetrazolium, inner salt (MTS) and the electron coupling reagent, phenazine ethosulfate. MTS reacts with cells to form formazan crystals in culture medium whose absorbance can be read at 490nm with a 96-well plate reader.

1 x 10^6 R1 cells were encapsulated in 1.5%HA – 3%PEGDA hydrogels and 1 x 10^6 R1 cells were seeded on bacteriological plates to promote EB formation in 2D cultures as described above. A set of blank 1.5%HA – 3%PEGDA hydrogels (without encapsulated cells) was made as a control. Cells and hydrogels were kept in culture at 37^{o}C, 5% CO_2 for 3 days. All hydrogel samples were transferred to separate wells of a 48-well tissue culture and 200 µl of R1 differentiation medium was added to each sample. 2D control cells were transferred to 15 ml centrifuge tubes and spun down at 4^{0}C, 300 x g for 5 minutes to obtain a tight pellet. The pellet was then resuspended in 200 µl of R1 differentiation medium and transferred to separate wells of a 96-well plate. 200 µl of R1 differentiation medium was added to three wells of the 96-well plate as a control. 40 µl of MTS solution was added to each 200 µl sample and allowed to incubate at 37^{0}C, 5% CO_2 for ~3 hours. Culture medium from the hydrogel samples was removed and transferred to the 96-well plate. Absorbance values were recorded at 490 nm with a 96-well plate reader (OpsysMR, Thermo Labsystems, Philadelphia, PA).

To analyze proliferation of encapsulated gels compared to 2D control cultures, a CFSE labeling was performed following the protocol provided by Molecular Probes™. Prior to cell encapsulation, predifferentiated R1 cells were labeled following trypsinization and cell pelleting. Pelleted cells were resuspended in warm PBS containing 0.1% bovine serum albumin (BSA) at a density of 1 x 10^6 cells per milliliter. A 5mM stock solution of CFSE in sterile DMSO was prepared and 2 μl of the stock solution was added per milliliter of cells in PBS. The cells were incubated at 37^0C, 5% CO_2 for 10 minutes, quenched with the addition of 5 volumes of cold R1 differentiation medium, and incubated on ice for 5 minutes. Cells were then pelleted and washed three times with cold R1 differentiation medium. Cells were then resuspended and utilized for cell encapsulation in 1.5%HA-3%PEGDA hydrogels as well as 2D cultures. Unlabelled hydrogel cultures, 2D cultures, and undifferentiated R1 cells were used as negative controls. Labeled undifferentiated R1 cells were used as a positive control.

Cells were released from hydrogels through degradation in ~2.5 milliliters of a 2,000 U/ml hyaluronidase (Sigma-Aldrich, St. Louis, MO) solution overnight. Cells were pelleted, rinsed twice with FACS buffer (described in section 3.6.2), resuspended in ~300 μl FACS buffer, and transferred to FACS tubes. 2D cultures were transferred to 15 ml centrifuge tubes and pelleted. These cells were rinsed once with PBS before the addition of ~400 μl of Accumax (Innovative Cell Technologies, San Diego, CA). EBs were incubated at 37^0C in Accumax for approximately 1 hour before the reaction was stopped with the addition of 1 milliliter of R1 differentiation medium. The EBs were vigorously pipetted 10-20 times and then filtered through a 40 μm mesh to obtain a single cell suspension. Single cells were then rinsed twice with FACS buffer, resuspended in ~300 μl of FACS buffer, and transferred to FACS tubes. Undifferentiated R1 cells were labeled with CFSE following the protocol above on the day of FACS analysis. All samples were run on the FACS Calibur in the Core facility (University of Texas Core Facility).

3.6 Hematopoietic stem cell marker analysis

3.6.1 Collection of cells and EBs from HA-PEGDA hydrogels

EBs were collected from 2D cultures by transferring the EB-media solution to 15 ml centrifuge tubes and incubating at 37^0C, 5% CO_2 for 30 minutes to allow EBs to fall to the bottom of the tube. The supernatant was then removed and the EB pellet was washed with 1 milliliter of PBS. The EB-PBS solution was allowed to incubate at 37^0C, 5% CO_2 for 15 minutes to allow EBs to collect at the bottom of the tube again. EBs underwent an Accumax treatment as described in section 3.5.2. The 40 μm same mesh was used for multiple samples of the same condition and the mesh was washed with 1 milliliter of medium or PBS between samples. The single-cell solution was transferred to a 15 ml centrifuge tube and kept on ice until trypan blue staining and cell counting with a hemocytometer.

Cells and EBs were collected from hydrogels through enzymatic degradation as described above. Released cells and EBs were pelleted and rinsed once with PBS. 300 μl of Accumax was added to each pellet and allowed to incubate for ~ 1 hour at 37^0C. The reaction was stopped with 1 milliliter of R1 differentiation medium and single-cell suspensions were obtained with a 40 μm mesh as described above. Single-cell solutions were again transferred to 15 ml centrifuge tubes and kept on ice until trypan blue staining and cell counting with a hemocytometer was performed.

3.6.2 FACS staining and analysis

Cells were stained for the surface markers, c-kit and sca-1 (BD Pharmingen), as well as for the intracellular marker Oct-3/4 (R&D Systems, Minneapolis, MN). Cells were also stained with isotype controls for the three markers (BD Pharmingen). A minimum of 2 x 10^5 cells are necessary for flow cytometry. To ensure this number of cells was obtained from each sample, cell numbers from all samples were obtained. To create FACS controls, extra cells from all samples were pooled and aliquotted to make FACS controls. The following separate FACS controls for cells released from hydrogels and 2D cultures were created: single-stained, unstained, and isotype controls. Cells from each sample were pelleted and then washed twice with cold FACS buffer (1% BSA, 0.05% Sodium Azide in PBS). After the first wash, samples were transferred to 1.5 ml or 2.0 ml microcentrifuge tubes. Following the second wash, samples were resuspended in ~ 50 µl of FACS buffer before proceeding with cell surface marker staining.

Samples were first blocked on ice for 10 minutes to prevent non-specific antibody binding by adding 1 µl of FcBlock (BD Pharamingen) to each sample. 1 µl of antibodies for ckit-APC and sca-1-PE was then added to each sample in dark conditions and allowed to incubate on ice for 30 minutes. Isotype control antibodies were added to the isotype control samples in the same manner. If no intracellular staining was performed, samples were washed twice with 500 µl of ice-cold FACS buffer and resuspended in 150 µl FACS buffer. Cells were then fixed by adding 150 µl of 2% paraformaldehyde to each sample and transferring samples to FACS tubes. Samples were stored in the dark at 4^0C until flow cytometry was performed.

For intracellular marker staining an intracellular staining kit (eBioscience) was used and a modified version of eBioscience's protocol was followed. After cell surface marker staining was completed, each sample was washed once with 1 ml of ice-cold FACS buffer. The supernatant was poured off and the remaining volume and cell pellet were pulse vortexed. 900 µl – 1 ml of Fixation/Permeabilization solution was added to each sample and incubated at 4^0C for ~45 minutes. Samples were then washed twice with 1.5 mls 10x Permeabilization Buffer or once with 4 mls of Permeabilization buffer. 1 µl of the Oct-3/4 antibody was then added to each sample and incubated on ice for 30 minutes. Samples were then washed twice with 500 µl FACS buffer and resuspended in a final volume of 300 µl before transferring to FACS tubes. All samples were stored in the dark at 4^0C until flow cytometry was performed.

3.7 Gene expression analysis

3.7.1 RNA isolation and DNase treatment

RNA was isolated from cell samples using TRIzol™ (Invitrogen, Carlsbad, CA) and the protocol provided by Invitrogen. Briefly, cells and EBs released from degraded hydrogels were pelleted and the supernatant was removed. 1 milliliter of TRIzol™ reagent was added to the cell pellets, pipetted several times to assist in chemical lysing of cells, and incubated for 5 minutes at room temperature to assure cell lysing. The lysed cells were stored in 1.5 milliliter nuclease-free microcentrifuge tubes at -80^{0}C before proceeding with RNA extraction. To separate organic phases from aqueous phases a phenol-chloroform extraction was performed. Briefly, 200 µl of chloroform was added to each sample and incubated at room temperature for 2-3 minutes. Samples were centrifuged at 12,000g, 4^{0}C for 15 minutes followed by transfer of the aqueous phase to separate 1.5 milliliter nuclease-free microcentrifuge tubes. 500 µl of isopropanol was then added to the samples and centrifuged as above to pellet the RNA. 1 milliliter of 75% ethanol was added to wash all RNA samples. After centrifugation at 7,500 x g for 5 minutes, the ethanol was poured off and RNA pellets were allowed to air dry for up to 30 minutes. Dried pellets were resuspended in 10 µl of nuclease-free water.

To remove any DNA from the RNA samples a DNase treatment was performed using the TURBO DNase kit (Ambion, Austin, TX). The protocol provided by the company was followed. Briefly, 1 µl of TURBO DNase buffer was added to each RNA sample followed by the addition of 1 µl of the TURBO DNase enzyme. Samples were transferred to 0.5 milliliter nuclease-free microcentrifuge tubes and were then placed in a 37^{0}C water bath and allowed to incubate for approximately 25 minutes. To stop the enzymatic reaction, 1.1 µl of the DNase inactivation reagent was added. Samples were centrifuged at 10,000 x g for 90 seconds. The aqueous supernatant was removed (~ 7 – 10 µl) and transferred to new 0.5 milliliter nuclease-free microcentrifuge tubes. Quantity and purity of RNA was assessed after this treatment using the Nanodrop (ND-1000, University of Texas Core Facility).

3.7.2 Real-time polymerase chain reaction

Equal quantities of RNA for each sample were reversed transcribed using a cDNA synthesis kit (SABiosciences, Frederick, MD). For real-time polymerase chain reaction (RT-PCR), 0.5 µl of primers for cKit and sca-1 were added to 7.5 µl RT^2 SYBR Green ROX Master Mix (SABiosciences, Frederick, MD), 6.0 µl dH_2O, and 0.75 µl cDNA. Each 15 µl sample was pipetted into a 386-well PCR plate and cycled using the following program on the ABI 7900HT RT-PCR machine (University of Texas Core Facility): 1 cylce for 10 minutes at 95^0C, 40 cycles for 15 seconds at 95^0C followed by 1 minute at 60^0C. Threshold values were obtained using SDS 2.2.1 software (Applied Biosystems, Foster City, CA).

3.7.3 Real-time polymerase chain reaction microarray analysis

RNA was isolated as described above and the protocol provided by SABiosciences Corporation was followed. Briefly, synthesized cDNA was diluted in 91µl of nuclease-free water and mixed with 1275 µl RT^2 SYBR Green ROX Master Mix and 1173 µl dH_2O. 25 µl of solution was added to each well of the 96-well Mouse Embryonic Stem Cell RT^2 Profiler™ PCR Array. The same RT-PCR machine, cycling program, and gene expression analysis software as above was utilized.

Chapter 4: Results and Discussion

4.1 Hydrogel chemical and physical characterization

4.1.1 Proton Nuclear Magnetic Resonance of Methacrylated HA

Proton nuclear magnetic resonance (^{1}H-NMR) was conducted on MeHA to verify methacrylation of HA. A ^{1}H-NMR was also performed on HA to serve as a reference spectra. The percent methacrylation of each reaction was calculated by taking the ratio of methacrylated molecules to the total number of disaccharide units. Total number of disaccharide units was found by summing the integral of the methyl peaks (~1.7-1.9 ppm) and dividing by 3, the number of protons associated with the HA methyl groups. Total number of methacrylate groups was calculated by summing the integral of the alkene protons (~5.2-5.5 ppm) and dividing by 2. To obtain percent methacrylation, the ratio was multiplied by 100.

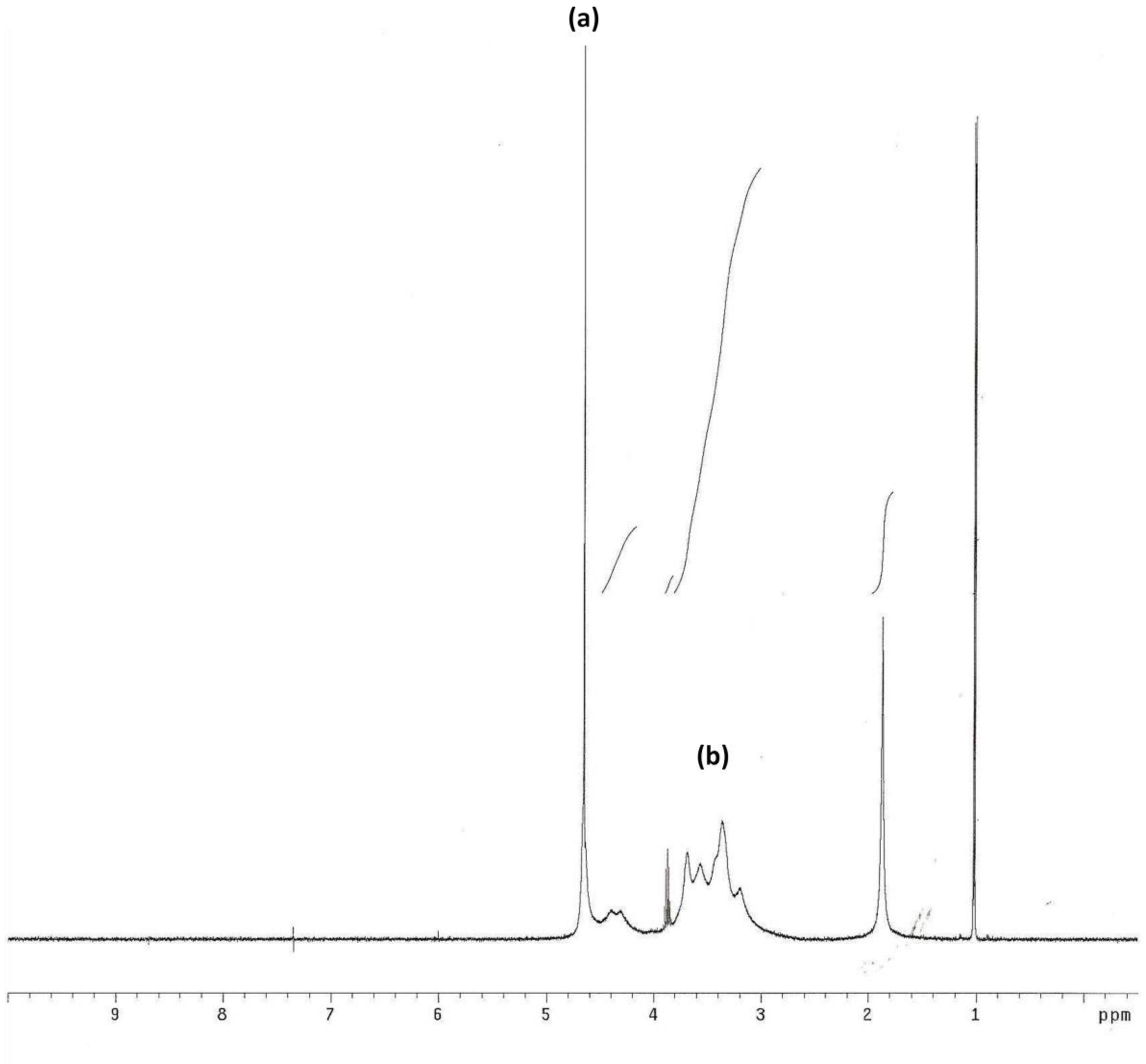

Figure 4-1. ^{1}H-NMR of Native Hyaluronic Acid. Hyaluronic Acid (MW ~ 2 x 10^6) (a) peak associated with the solvent D_20; (b) peak associated with the disaccharide unit.

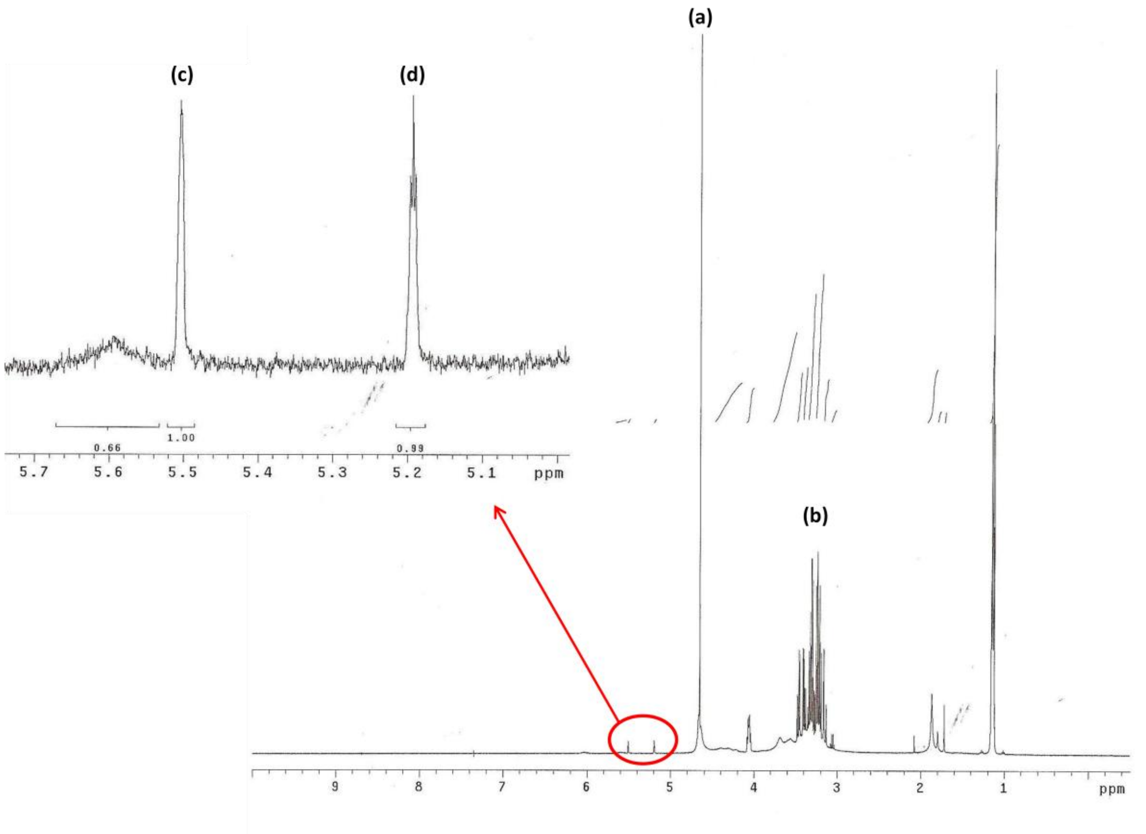

Figure 4-2. ^{1}H-NMR of Methacrylated Hyaluronic Acid. (a) peak associated with the solvent D_20; (b) peak associated with the disaccharide unit; (c and d) peaks associated with the methacrylate groups (~ 5.2 – 5.5 ppm).

Figures 4-1 and 4-2 are the NMR spectra of unmodified HA and MeHA respectively. These spectra are comparable to those published by Leach *et. al.*.[38] Peak "a" on both NMR spectra is associated with the solvent D_2O. Peaks labeled "b" on both spectra correspond to protons of the disaccharide unit. Methacrylate groups will shift downfield on the NMR. As shown in the Figure 4-2 inset, two peaks labeled "c" and "d" have shifted downfield (~5-6 ppm) in comparison to unmodified HA indicating successful methacrylation. Table 4-1 shows the range of percent methacrylation obtained in separate reactions. Percentages ranged from ~9% - 30% which is consistent with values obtained by Leach *et. al.*.[38]

Table 4-1. Percent Methacrylations from Separate HA Methacrylation Reactions

Sample	Methyl Peaks	Alkene Protons	Percent Methacrylation
Apr-08	3.21	1.00	31.20%
Jul-08	11.1	1.04	9.35%
Apr-09	8.26	0.995	12.00%

4.1.2 Determination of degradable hydrogels and degradation profiles

In order to observe the affects of the synthetic, biomimetic microenvironment on the encapsulated mESC surface markers, a degradable hydrogel system was required. Furthermore, it was necessary to develop a system which degraded in 24 hours or less to minimize mESC exposure to factors outside of the hydrogel system. Initial studies were conducted to determine HA hydrogels and HA-PEGDA co-gels which met this specification. An enzyme solution with a concentration of 2,000 U/ml of hyaluronidase in growth medium was added to the gels and incubated at 37^0C for 24 hours. Table 4-2 shows the hydrogel formulations which were shown to be degradable in this time period. Increasing HA above 2% (w/v) created an extremely viscous solution incapable of being pipetted. Increasing PEGDA concentrations above 3% (w/v) produced hydrogels which were not degradable in the 24 hour time period. These results are consistent with those of Wieland *et. al.* who found that co-gels composed of HA-acryl and more than 4% (w/v) 4-arm PEG-acryl were considered “mechanically stable” for more than 50 days under enzymatic conditions [40]. Only the hydrogel formulations listed in Table 4-2 were used in the remaining studies.

Table 4-2. Degradable HA Hydrogel and HA-PEGDA co-gel Formulations

HA (%)	PEGDA (%)
1	0
1.5	0
2	0
1	2
1	3
1.5	2
1.5	3

To fully characterize the behavior of the hydrogels under enzymatic conditions, degradation studies were performed. Figures 4-3 and 4-4 show the results of degradation studies. Pure HA hydrogels and HA-PEGDA co-gels have significantly different degradation profiles. Degradation times of pure HA gels ranged between 1.25 and 2 hours while co-gels took between 6 and 16 hours to fully degrade. An unpaired, two-tailed student's t-test was performed at each time point to determine if the degradation profiles of pure HA hydrogels and HA-PEGDA co-gels were significantly different ($p < 0.05$). 1%HA gels were the fastest to degrade and the degradation profile appears to be exponential in comparison to 1.5%HA and 2.0%HA whose profiles appear more linear. 1.5%HA and 2.0%HA degrade in very similar fashions and their error bars at each time point overlap suggesting that the degradation behaviors of these two gels is not significantly different. This was confirmed by examining the p values of 1.5%HA and 2.0%HA hydrogels at each time point. The masses of both hydrogel formations at all time points were not found to be significantly different. A statistical comparison of masses corresponding to 1%HA and 2.0%HA hydrogels also showed no significant difference. The only statistically significant difference was found between 1.5%HA and 1%HA hydrogels at two time points (0.5 hours and 0.75 hours). Statistical comparison of the degradation profiles indicates that overall, the formulation of pure HA hydrogels does not significantly alter the degradation profiles. The profiles are statistically similar with the exception of two time points.

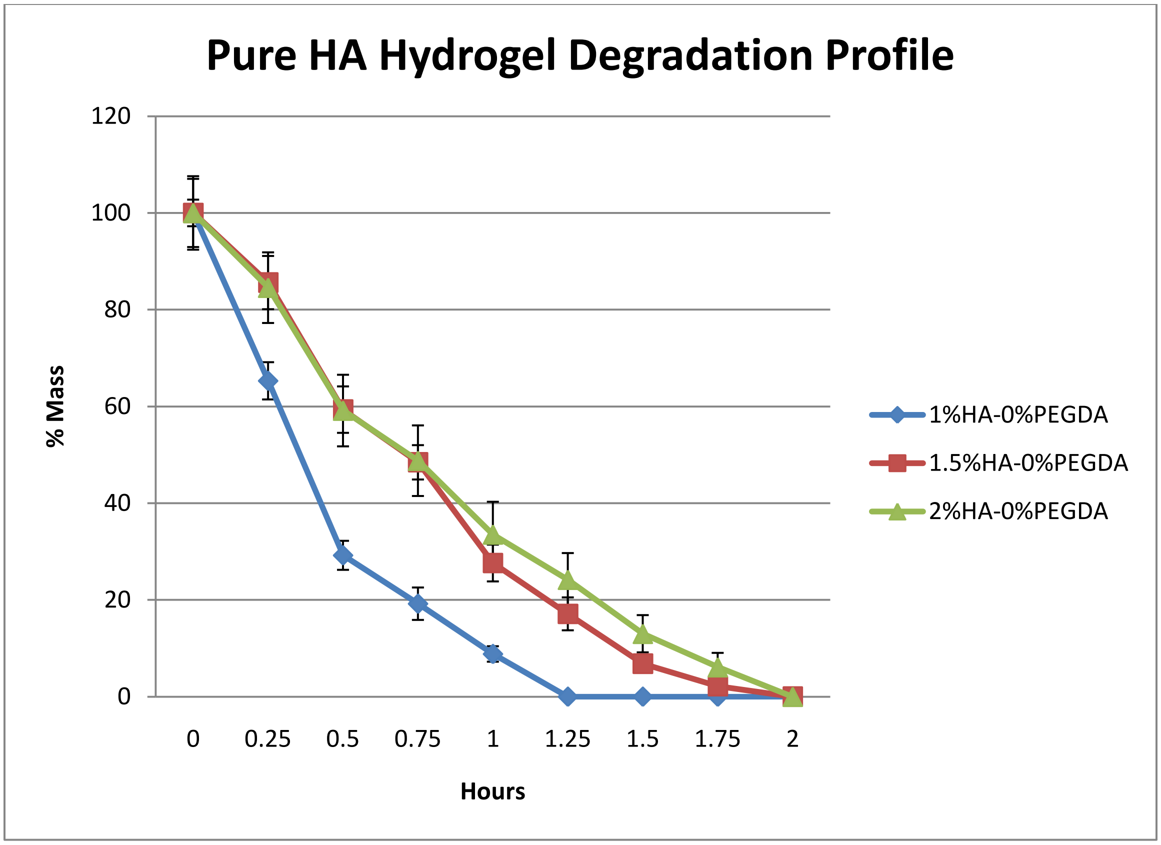

Figure 4-3. ***In Vitro*** **Degradation profile of pure HA hydrogels.** Degradation profiles of pure HA hydrogels incubated in 2,000 U/ml hyaluronidase at 37^{0}C. Masses were measured every 0.25 hours until complete degradation occurred. Each data point is an average value ± standard error (n = 4).

At the first time point in the co-gel degradation profile (1 hour) all the co-gels appear to degrade in the same manner. This observation was confirmed with a p value < 0.05 comparing all hydrogels. In following time points, the co-gels differentiate themselves. Co-gel degradation profiles show a difference in behavior between co-gels containing 2% (w/v) PEGDA and co-gels with 3% (w/v) PEGDA. Statistical comparison of 2% (w/v) co-gel masses, revealed no significant differences at any time point. The degradation profiles of 2% (w/v) co-gels cannot be considered different. In examining profiles associated with 3% (w/v) co-gels, statistical analysis at each time point indicated no difference in the hydrogel masses. The degradation profiles of 3% (w/v) co-gels are also not different..

There is a significant difference ($p < 0.05$) between 2% (w/v) and 3% (w/v) co-gels. Between hour 2 and hour 9, the degradation profiles of 2% (w/v) co-gels and 3% (w/v) co-gels are different. The degradation profile of 1%HA-3%PEGDA co-gels can be considered the same as 2% (w/v) co-gels from hour 10 until hour 16. From hour 14 until full co-gel degradation at hour 16, the degradation profiles of all co-gels can be considered the same ($p > 0.05$).

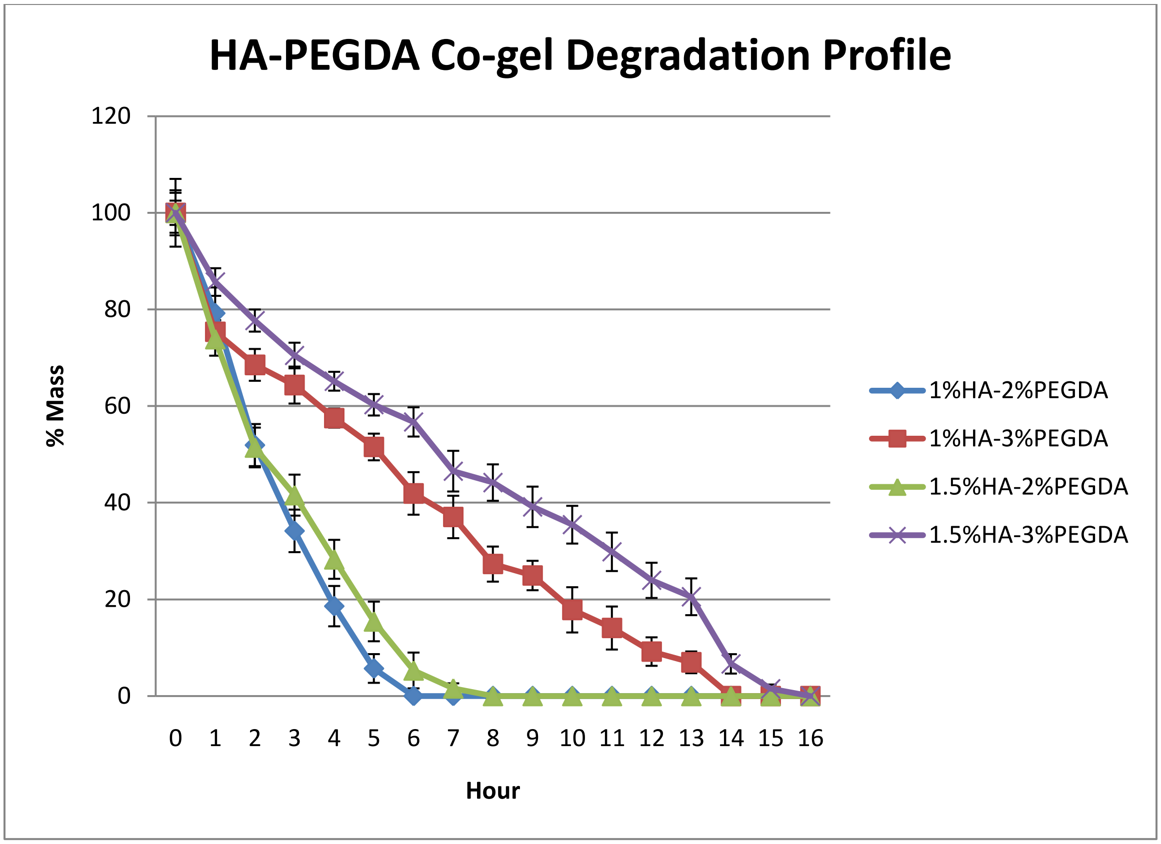

Figure 4-4. *In Vitro* Degradation profile of HA-PEGDA co-gels. Degradation profiles of HA-PEGDA co-gels in the presence of 2,000 U/ml hyaluronidase at 37^{0}C. Masses were measured every hour until complete degradation occurred. Each data point is an average value ± standard error (n = 4 except for 1%HA-2%PEGDA which has n = 3).

An apparent trend in the data is an increase in PEGDA results in slower degradation. The enzyme, hyaluronidase, only cleaves the bond between the disaccharide units of HA. Crosslinks created in pure HA gels are only between the functional groups of HA molecules. The introduction of PEGDA into hydrogels creates more opportunities for crosslinks between HA functional groups and PEGDA functional groups. HA gels will degrade quickly because all the crosslinks contains molecules which will be enzymatically cleaved. Co-gels will take longer to degrade because not all the crosslinks will contain HA molecules. Moreover increasing PEGDA quantities increases the possibility of crosslinks between PEGDA molecules and therefore will lengthen the amount of time for full degradation. Most importantly, this data indicates in detail that all of these hydrogel systems degrade in the desired time of 24 hours or less.

4.1.3 Swelling Ratios

More than half of the hydrogels formulated contain more than one component and therefore, pore size cannot be directly calculated. A swelling study, another method of characterizing pore size, was conducted to calculate the swelling ratio of the different hydrogels. The swelling ratio (Q) was calculated using the formula, $Q = \frac{Ms}{Md}$. An unpaired, two-tailed student's t-test was performed to determine statistically significant differences ($p < 0.05$) in swelling ratios between gels. Figure 4-5 shows the results of the swelling study.

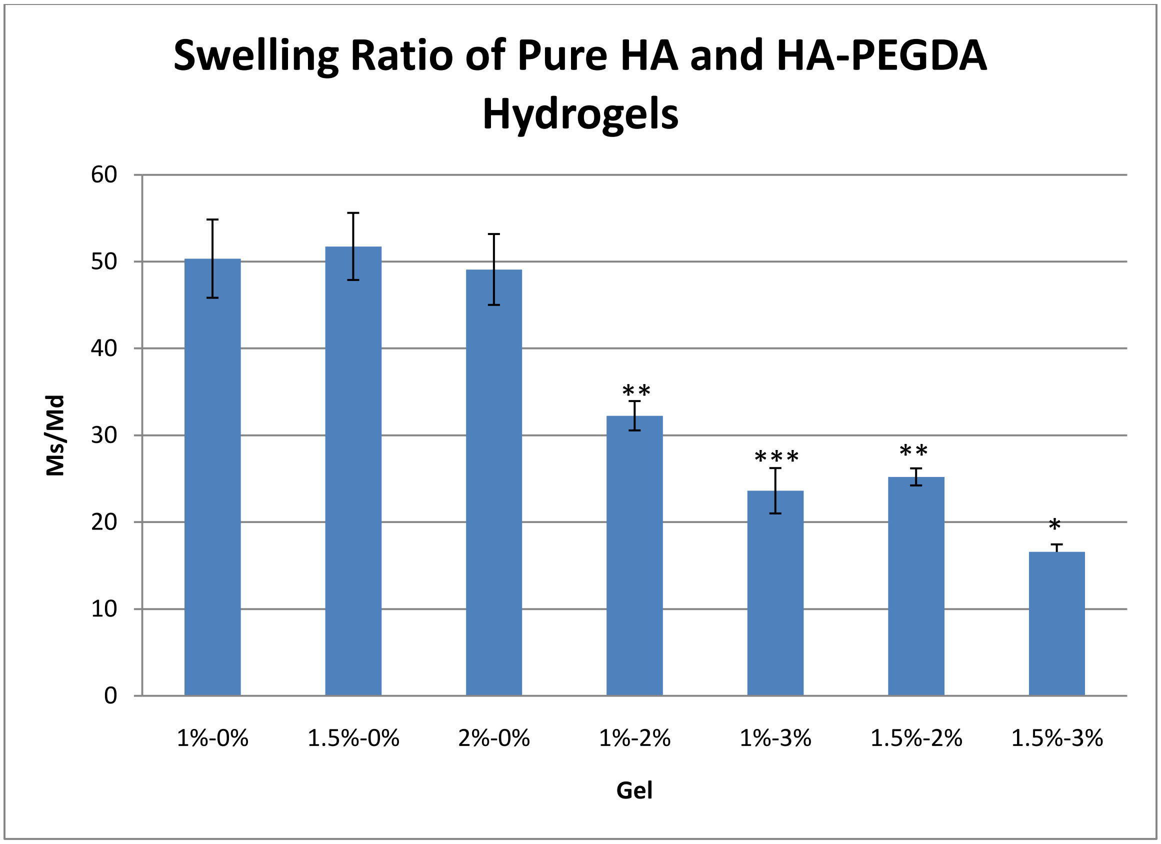

Figure 4-5. Swelling Ratio of HA hydrogels and HA-PEGDA co-gels. Swelling ratio is a method of characterizing the degree of crosslinking and pore sizes in multi-component hydrogels. The swelling ratio was determined by dividing the swollen mass by the dried mass. (*) swelling ratio significantly lower than all pure HA gels and HA-PEGDA co-gels; (**) swelling ratio significantly different from all hydrogels except 1%HA-3%PEGDA; (***) swelling ratio significantly lower than all hydrogels except 2% (w/v) co-gels. Each data point is an average value ± standard error (n=4 for all hydrogels except 1%HA and 1%HA-3%PEGDA which have n=3).

All of the pure HA gel swelling ratios were significantly different from all the co-gel swelling ratios indicating pure HA gels are not as tightly crosslinked and are able to imbibe more water. Co-gel swelling ratios are lower than those of pure HA gels because of the addition of high molecular weight PEGDA. An apparent trend in the data suggests that the introduction of PEGDA (MW 3400) into the polymer solutions allows for an increase in crosslinks and a tighter mesh network. This decreases the pore sizes of the hydrogel network and results in a decrease in water intake.

Both of the co-gels containing 2% (w/v) PEGDA have a swelling ratio which is significantly different from all of the formulated hydrogels with the exception of 1%HA-3%PEGDA. Similarly, the 1%HA-3%PEGDA co-gel swelling ratio is significantly different from all the formulated hydrogels except the co-gels containing 2% (w/v) PEGDA. The swelling ratios of the 2% (w/v) co-gels and 1%HA-3%PEGDA hydrogels cannot be considered different indicating that their composition was not altered enough to significantly change the mesh network size. Only the 1.5%HA-3%PEGDA co-gel has a swelling ratio which is significantly different from all formulated hydrogels. These results indicate that swelling ratio is not solely dependent on PEGDA quantities. Crosslinking of the two polymers is due to the presence of functional groups on both the synthetic and natural polymers (acrylate and methacrylate groups). Therefore, the largest increase in both HA and PEGDA quantities will result in the tightest crosslinking.

4.1.4 Scanning electron microscopy

Figure 4-6 contains SEM images of dried 1.5%HA-3%PEGDA (a-d) co-gels and 1.5%HA hydrogels (e-f). To obtain these images, hydrogels were dried in two fashions: freeze-drying and ethanol dehydration. Images a-b were prepared through an ethanol dehydration method as described in materials and methods. Images c-f were dried through lyophilization for ~24 hours. These images illustrate the porous nature of these hydrogels. The swelling ratios of HA gels and HA-PEGDA co-gels suggest that HA gels should be more porous however, the images in this figure do not seem to correspond to that finding. This could be due to the method of drying utilized. Lyophilization will disrupt the true molecular interactions and structure in a relaxed or swollen gel. The molecular interactions in the HA gel could have been disrupted and therefore the SEM images may not be truly representative of HA hydrogel porosity. Also, as described in the background, the super-swelling property of HA is a result of water's interaction with H-bonds between polymer chains; the HA hydrogels' swelling ratios are not solely dependent on porosity.

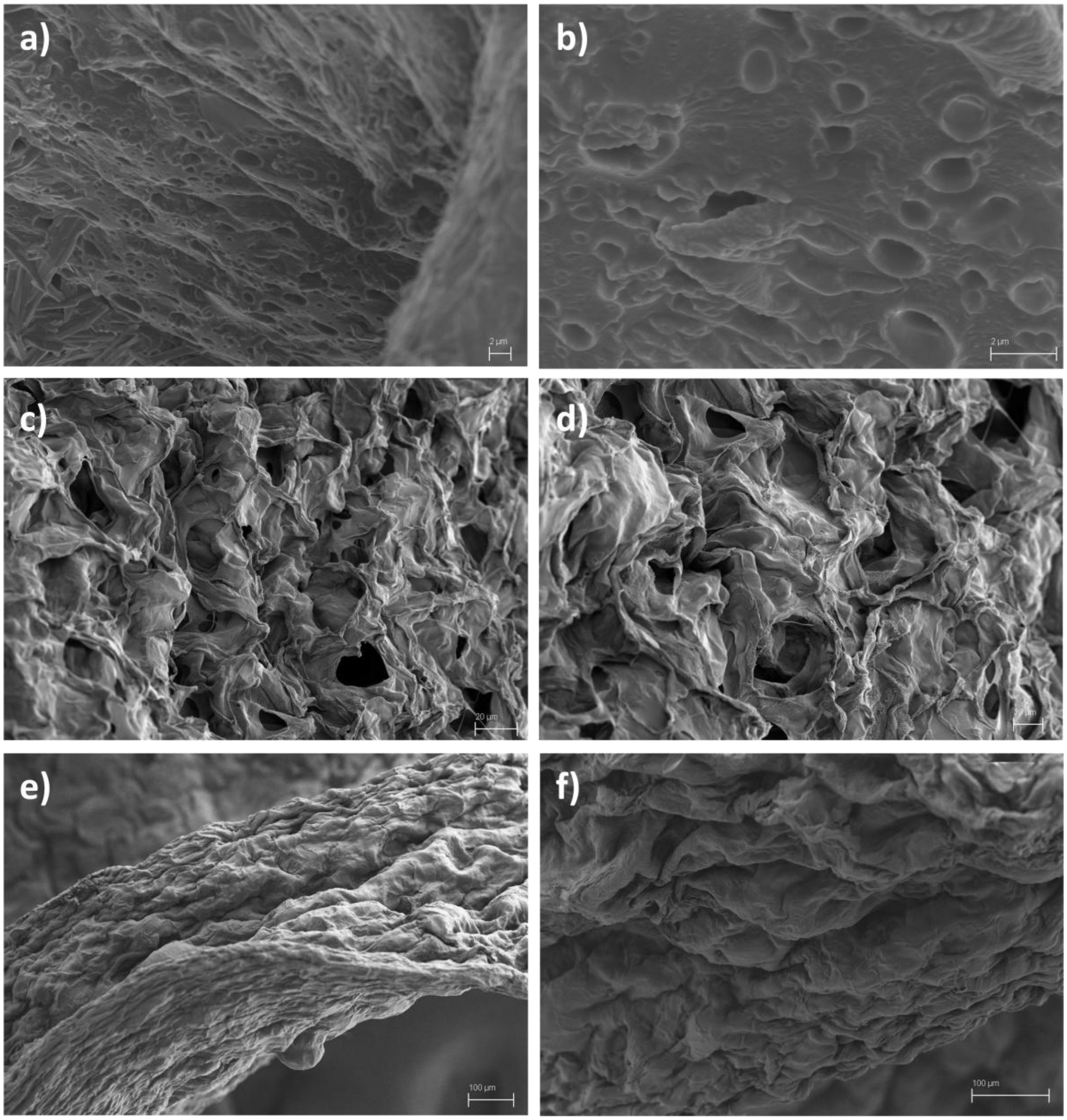

Figure 4-6. SEM images of Dried HA hydrogels and HA-PEGDA co-gels. (a and b) 1.5%HA-3%PEGDA hydrogels dried using ethanol dehydration and sputter-coated with Ir; (c and d) lyophilized 1.5%HA-3%PEGDA hydrogels sputter-coated with Pt-Pl; (e and f) lyophilized 1.5%HA hydrogels sputter-coated with Pt-Pl.

4.1.5 Compressive modulus

A compressive modulus study was done to determine the mechanical stability of the hydrogels. Figure 4-7 contains the results of this study. An unpaired, two-tailed student's t-test was performed to determine statistically significant ($p < 0.05$) differences in each hydrogel's mechanical strength. There was a significant difference between 1.0%HA and 1.5%HA gels with 1.0%HA having a significantly lower modulus. This is most likely a result of increased crosslinking in 1.5%HA gels imparting more mechanical strength on the gel. The only statistically significant co-gels were 1.5%HA-2%PEGDA and 1.5%HA-3%PEGDA gels. The composition of these gels only differs by 1% (w/v) PEGDA therefore, our expectation was that the compressive modulus would not be significantly different. The p-value obtained for this pairing was borderline ($p = .047$). The variances for the groups are so large and the compressive modulus values are too broadly distributed to conclusively say, with a small number of tests, that these groups are definitively different.

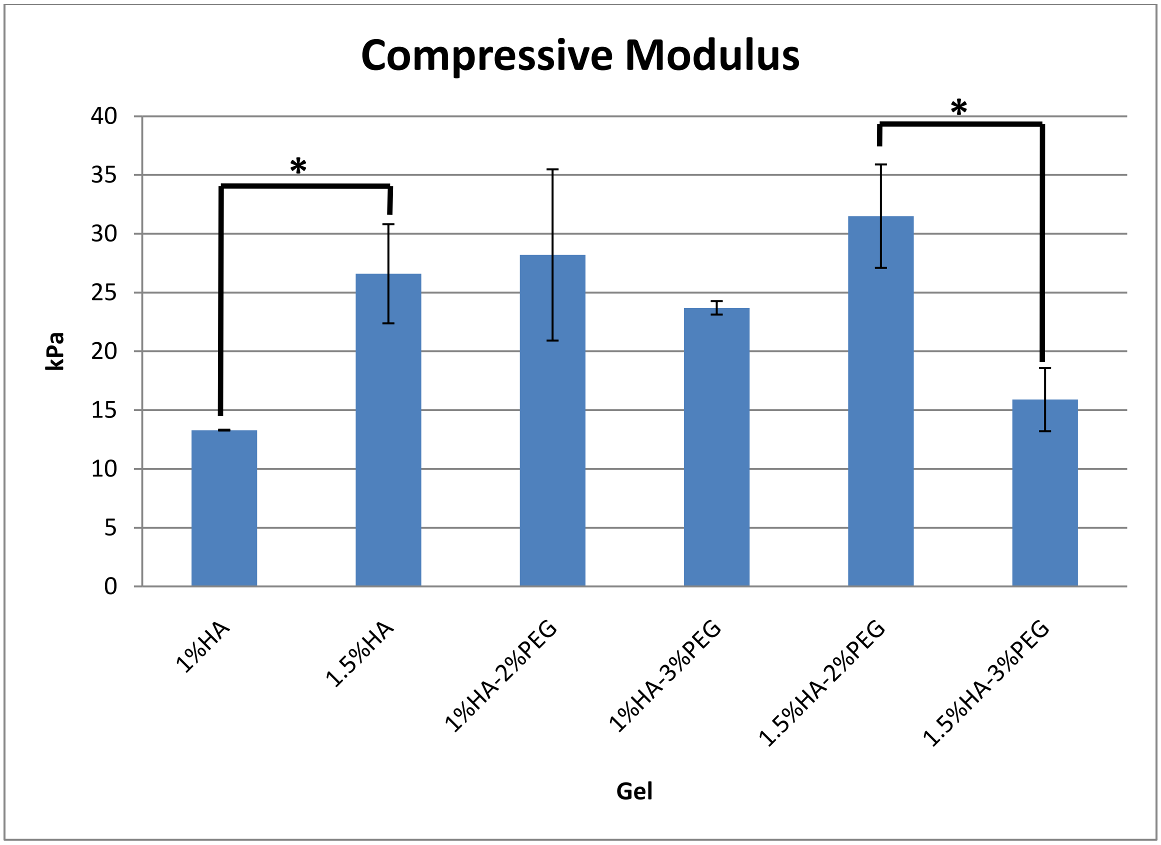

Figure 4-7. Compressive Modulus measurements of HA hydrogels and HA-PEGDA co-gels. (*) The compressive modulus of 1%HA hydrogels was found to be significantly lower ($p < 0.05$) than 1.5%HA hydrogels. Similarly, the compressive modulus of 1.5%HA-3%PEGDA was significantly lower ($p < 0.05$) than 1.5%HA-2%PEGDA. Each data point is an average value ± standard error (n=4 for 1.5%HA and 1.5%HA-3%PEGDA; n=3 for 1%HA, 1%HA-3%PEGDA, and 1.5%HA-2%PEGDA; n=2 for 1%HA-2%PEGDA).

4.2 Encapsulated cell viability and proliferation

4.2.1 MTS assay

A calorimetric MTS assay was conducted to measure cell proliferation in the hydrogel system (1.5%HA-3%PEGDA) and 2D cultures treated with UV (UV-2D) compared to 2D control cultures. Figure 4-8 illustrates the optical density (OD) measurements obtained. OD measurements of plain media or HA-PEGDA co-gels without encapsulated cells were subtracted out of the remaining measurements to eliminate error from background signal. A standard curve could not be made due to the nature of the cells being cultured. mESCs cultured in a 2D environment form EBs, clusters of cells. To create a standard curve, cell quantities must be known and to count the cells in the 2D controls, the EBs must be disrupted by an enzymatic treatment (trypsin or accumax). The treatment process does not completely disrupt the EBs and it also results in a considerable amount of cell death (shown in cell viability data); cell counts obtained would not be accurate. Additionally the culture systems being assayed will not undergo any enzymatic treatment in an attempt to quantify proliferation in each culture system without introducing extrinsic factors.

To assign a quantitative cell proliferation value to OD measurements, an assumption was made. Since no extrinsic factors (i.e. UV light, polymer, photoinitiator) were introduced to the 2D control cultures, cell proliferation in this system was assumed to be 100%. The initial seeding density of each culture system was ~1×10^6 cells; therefore, percent proliferation for the hydrogels and UV-2D samples could be determined. Table 4-3 shows percent proliferation. An unpaired, two-tailed student's t-test was conducted to determine statistically significant ($p < 0.05$) differences between groups. As evidenced by the OD measurements, the decrease in cell proliferation in hydrogels compared to both 2D control cultures and UV-2D cultures is statistically significant. Although cell proliferation is reduced in the UV-2D samples compared to 2D controls, this difference is not statistically significant. These results suggest that multiple factors are responsible for the decline in encapsulated mESC proliferation. These factors could include exposure to free radicals from the photoinitiator and extensive pipetting with polymer solution. The restrictive nature of the hydrogel mesh network may also be responsible. There is no way to conclusively pinpoint the main source of reduced cell proliferation in the hydrogel system.

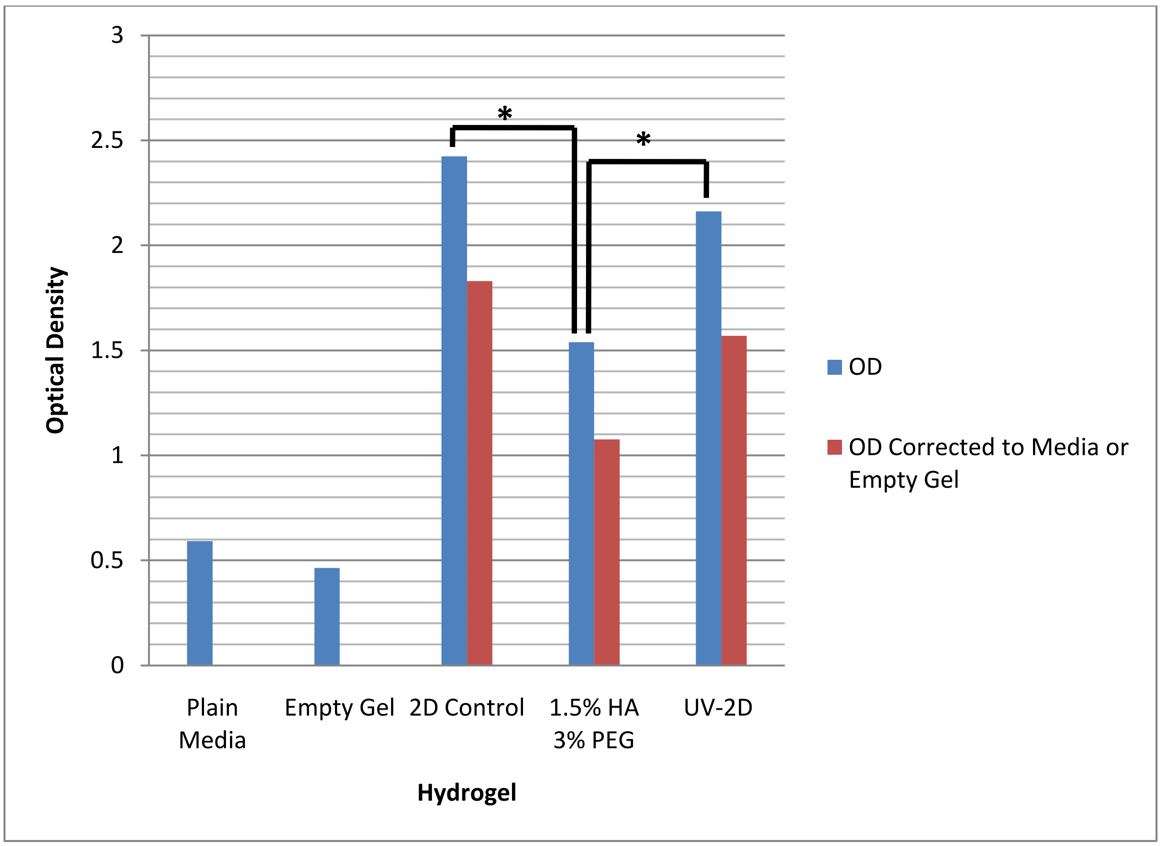

Figure 4-8. Optical density measurements obtained from MTS assay Optical density measurements from an MTS assay were obtained using a plate reader. The ODs of 2D controls and UV-treated 2D controls (2D-UV) were corrected by subtracting the OD of plain media. ODs of hydrogels were corrected by subtracting the OD of empty hydrogel controls. (*) The OD of a representative hydrogel (1.5%HA-3%PEGDA) was significantly lower ($p < 0.05$) than both 2D and 2D-UV samples. Each data point is an average value ± standard error (n=3).

Table 4-3. Percent Proliferation of Encapsulated mESCs

	2D Control	1.5%HA - 3% PEG	UV-2D
OD Corrected to Media or Empty Gel	1.83	1.08	1.57
Percent Proliferation	100	58.8	85.8

4.2.2 CFSE labeling

CFSE labeling of cells in 2D control cultures and hydrogel cultures was performed to acquire additional cell proliferation measurements. Analysis of labeling was done with flow cytometry. Figure 4-9 includes the FACS histograms of CFSE labeled 2D control cells (A) and CFSE labeled encapsulated mESC cells (B). Figure 4-10 shows the percentages of each cell population present in the histogram. An unpaired, two-tailed student's t-test was done to determine statically significant differences in cell population percentages.

The CFSE stain will appear around the 10^3 - 10^4 region of the histogram. As cells undergo mitotic division, they lose the CFSE labeling and cells without CFSE will appear in the 10^0 – 10^1 region of the histogram. Distinct cell populations can be seen on the histogram as more cells undergo mitosis and lose CFSE labeling. As illustrated in the FACS histograms (Figure 4-9), mESCs from the 2D controls proliferated to the point that CFSE was eliminated from the culture and only one cell population remained. Encapsulated mESCs did not proliferate as efficiently and three different populations are present in the culture.

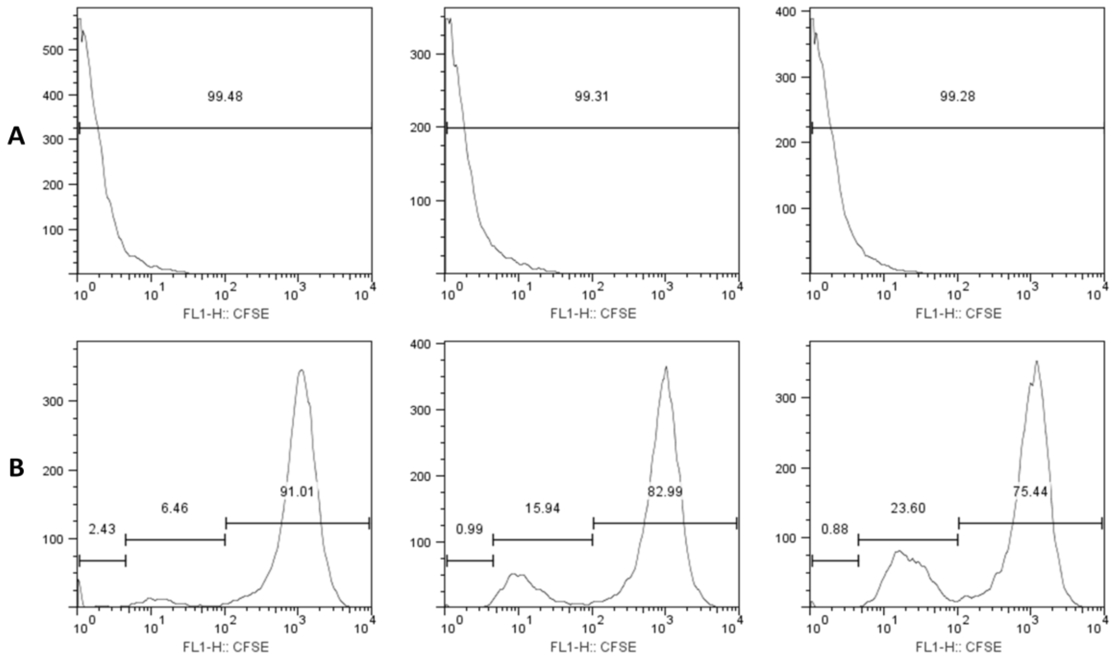

Figure 4-9. FACS histograms of CFSE labeled cell populations. (A) FACS histograms of 2D controls. (B) FACS histograms of a representative hydrogel (1.5%HA-3%PEGDA). Different peaks on the histograms are indicative of different cell populations. Cells retaining the CFSE labeling are found in $\sim10^3 - 10^4$ region. As cells proliferate and divide, the CFSE labeling diminishes. Cells which have undergone extensive proliferation are found in $\sim10^0 - 10^1$ region. 2D controls lost all CFSE labeling while the majority of hydrogel samples retained the CFSE labeling.

As demonstrated by both Figures 4-9 and 4-10, the largest of these populations is in the CFSE region of the histogram indicating that the majority of encapsulated mESCs did not proliferate. This again could be the result of a number of factors including steps taken during photopolymerization or the restrictive nature of the mesh network may not allow for proficient proliferation.

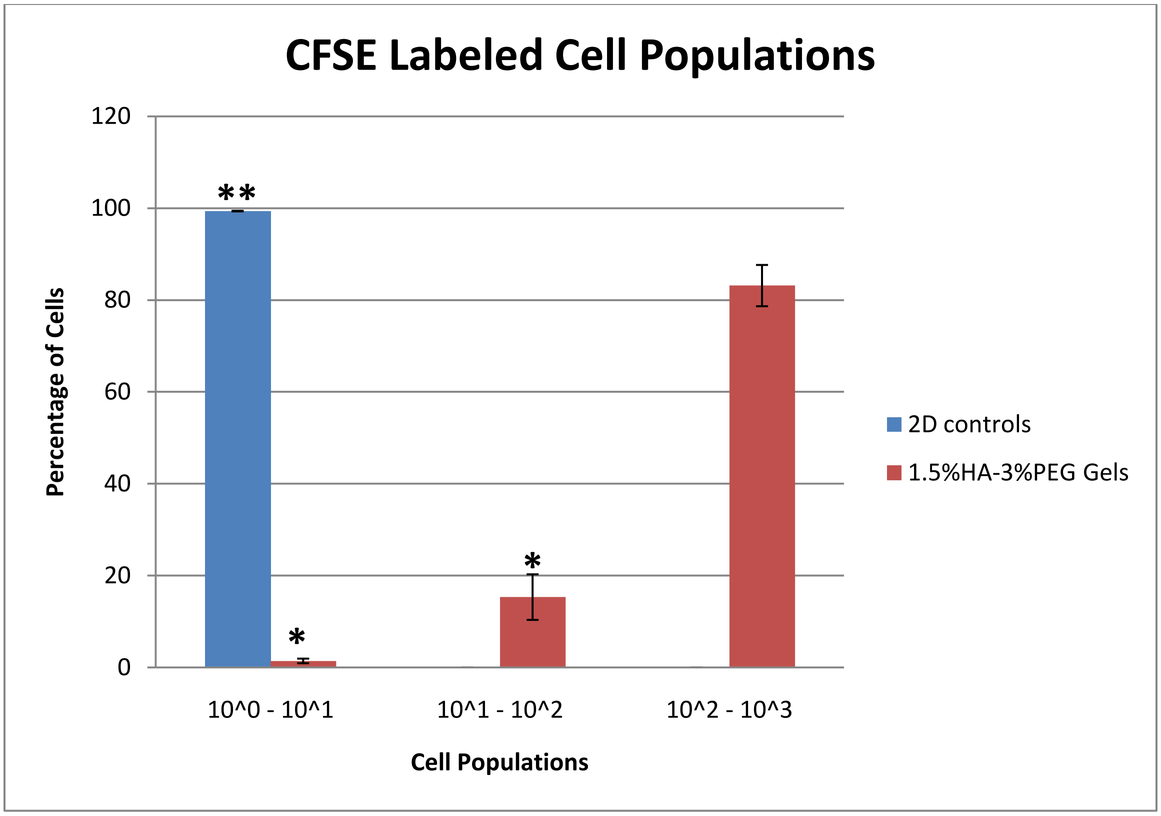

Figure 4-10. Summary of CFSE labeled cell populations. (*) CFSE labeled population significantly lower than 2D controls and 10^2 – 10^3 population of hydrogels; (**) 2D controls higher than all hydrogel populations. Each data point is an average value ± standard error (n = 3).

4.2.3 Propidium Iodide staining

To examine cell viability in hydrogel systems compared to 2D control cultures, a propidium iodide (PI) stain was conducted and analyzed with flow cytometry. An unpaired, two-tailed student's t-test was done to reveal statistically significant ($p < 0.05$) differences in cell viability. Figure 4-11 shows the cell viability results of cells after 3 days of culture. mESCs from 2D control cultures (2D_set1) and 1.5%HA-3%PEGDA hydrogel cultures (Gel_set1) were harvested and subjected to an Accumax treatment as described in materials and methods. MEF cells (positive control) and pre-differentiated mESCs were not subjected to an Accumax treatment. The percentage of live pre-differentiated cells compared to MEF cells was not statistically different; therefore, pre-differentiated mESCs, the precursor to 2D control and hydrogel cultures, can be considered the control group. The decrease in percentage of live cells in 2D control cultures and hydrogel cultures compared to pre-differentiated cells is statistically significant. This assay measures cell viability after enzymatic processing and consequently is not a completely accurate measurement of viability during the culture itself. It is rather a measurement of cell viability after creating a single-cell suspension which is of value in flow cytometric analysis.

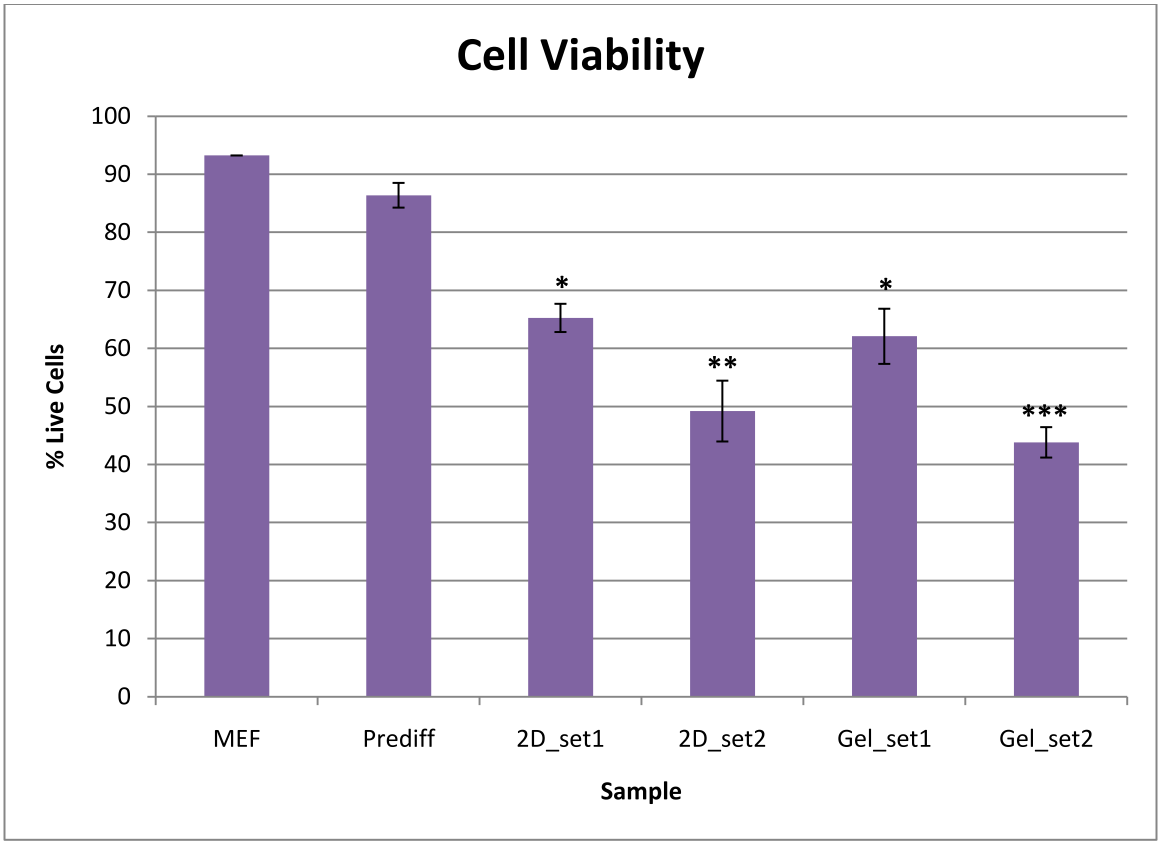

Figure 4-11. Percentage of Live Cells in 2D and hydrogel cultures. Cell viability was obtained by staining positive controls (MEF and R1 predifferentiated cells), 2D controls, and representative hydrogels (1.5%HA-3%PEGDA) with propidium iodide and analyzing with flow cytometry. 2D_set1 and Gel_set1 samples were subjected to Accumax enzymatic treatment. 2D_set2 and Gel_set2 were not subjected to Accumax enzymatic treatment. (*) Cell viability significantly lower ($p < 0.05$) than R1 predifferentiated cells; (**) Cell viability significantly lower ($p < 0.05$) than MEF and R1 predifferentiated cells; (***) Cell viability significantly lower ($p < 0.05$) than all samples. Each data point is an average value ± standard error (n=4 for all hydrogel samples; n=3 for positive controls and all 2D controls).

The effect of an enzymatic treatment with Accumax was also examined in this study. 2D_set2 and Gel_set2 were not subjected to Accumax. To obtain single-cell suspension for FACS analysis, these cells were vigorously pipette and put through a cell strainer. Figure 4-11 shows the decrease in live cell percentage in both these cultures compared to the positive controls and the Accumax treated cultures. 2D_set2 was only significantly different from the pre-differentiated control but the decreased live cell population in Gel_set2 was statistically significant from all samples except 2D_set2. These results suggest an Accumax treatment will significantly increase the quantity of live cells in hydrogel cultures after single-cell processing but will not increase the live cell population remaining in 2D cultures after processing.

4.3 EB formation in hydrogels

4.3.1 Light microscopy

Figure 4-12 displays light microscopy images taken to provide qualitative evidence of EB formation in the hydrogels at different time points (Day 2, Day 5). EB formation in 2D cultures was also imaged. In all culture conditions EB size increased from Day 2 to Day 5.

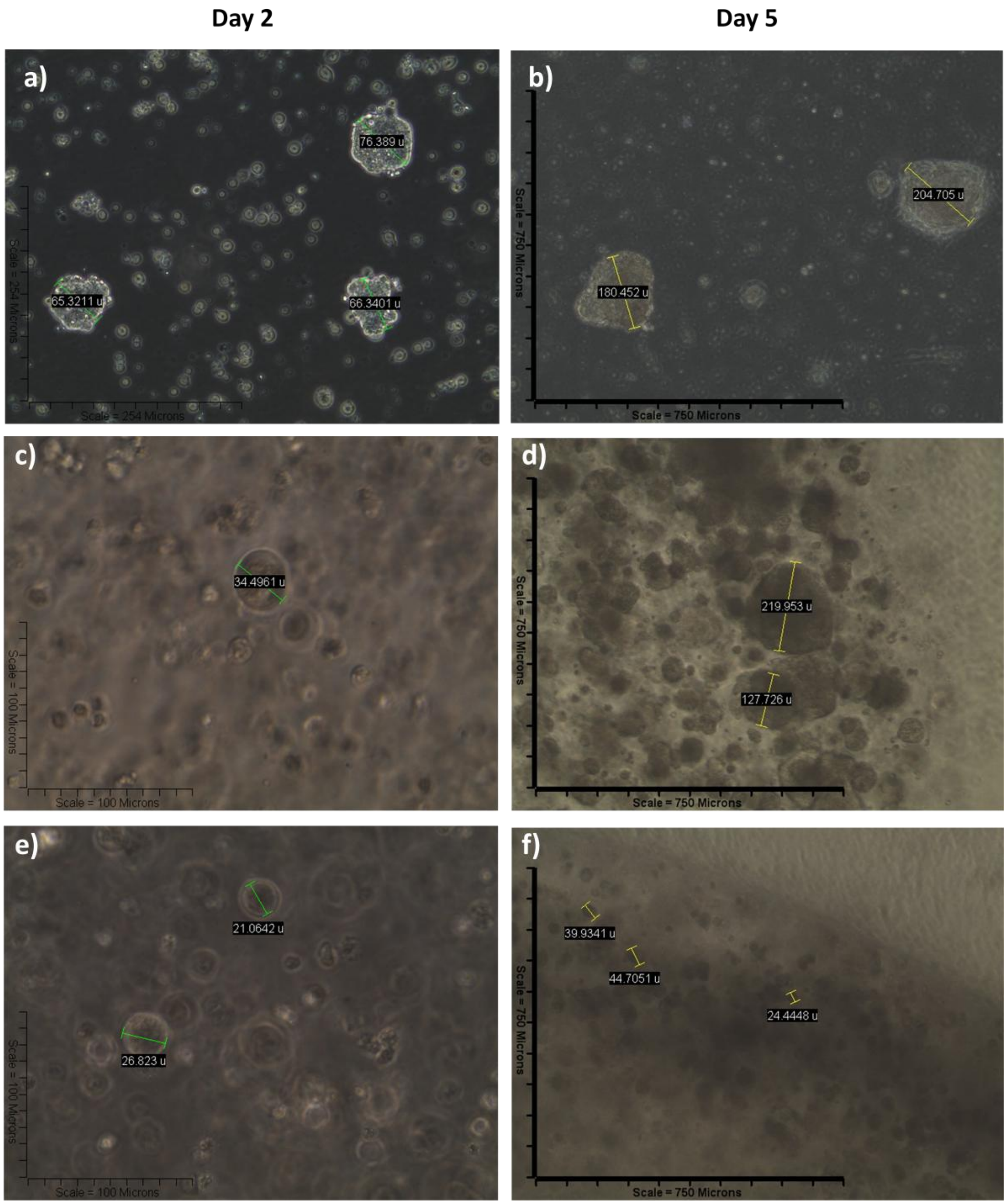

Figure 4-12. Light Microscopy images of EBs encapsulated in hydrogels. Representative hydrogels and 2D controls were imaged (10X magnification) on Day 2 and Day 5 post-encapsulation to monitor EB formation and size. (a and b) 2D controls; (c and d) 1.5%HA hydrogels; (e and f) 1.5%HA-3%PEGDA co-gels. 2D controls, hydrogels, and co-gels all have the same initial seeding density of 1 x 10^6 cells.

On Day 5 EBs of comparable sizes were observed between 1.5%HA hydrogel cultures and 2D control cultures indicating that differentiation was occurring in both culture systems. The size of EBs formed in the 1.5%HA-3%PEGDA co-gel culture was much smaller than those in the other systems. This is most likely due to the tight mesh network created with the addition of a high molecular weight PEGDA which restricts EB expansion. Figure 4-13 includes images of cells and EBs (Day 5) in the center of the hydrogels and demonstrates the inhibition of EB growth in the co-gel cultures in comparison to pure HA gel cultures. Another observation was the tendency of EBs to form near the edges of the hydrogels as shown in Figure 4-12. This is the region of the hydrogel with the least physical restriction and allows the EBs to expand and proliferate more than EBs captured in the mesh network in the hydrogel center.

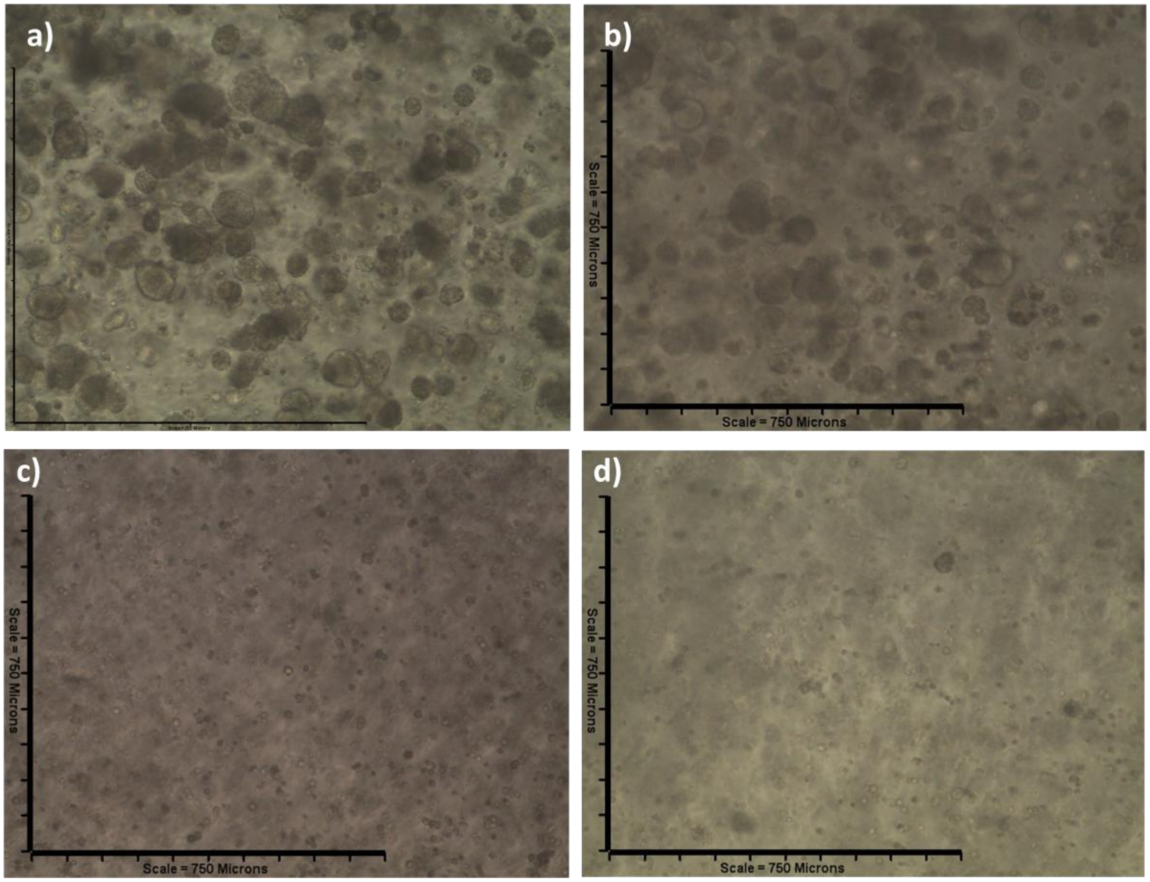

Figure 4-13. Light microscopy images of encapsulated mESCs at the center of hydrogels. Differences in EB formation and size was seen between pure HA hydrogels and HA-PEGDA co-gels. EBs tend to form on the edges of hydrogels were there is room for proliferation and expansion; the center of hydrogels restrict expansion. Pure HA hydrogels are less restrictive than co-gels which have a tighter mesh network as seen above. (a) 1%HA; (b) 1.5%HA; (c) 1%HA-3%PEGDA; (d) 1.5%HA-3%PEGDA. All images (10X magnification) were obtained on Day 5.

4.3.2 Scanning electron microscopy

SEM was also performed on dried hydrogels (1.5%HA-3%PEGDA) containing fixed, encapsulated mESCs after 7 days of culture. Images in Figure 4-14 show formation of EBs in the hydrogel. It was again observed that most of the EBs migrate towards or grow near the edges of the hydrogels. Images of these EBs were captured on the hydrogel surface.

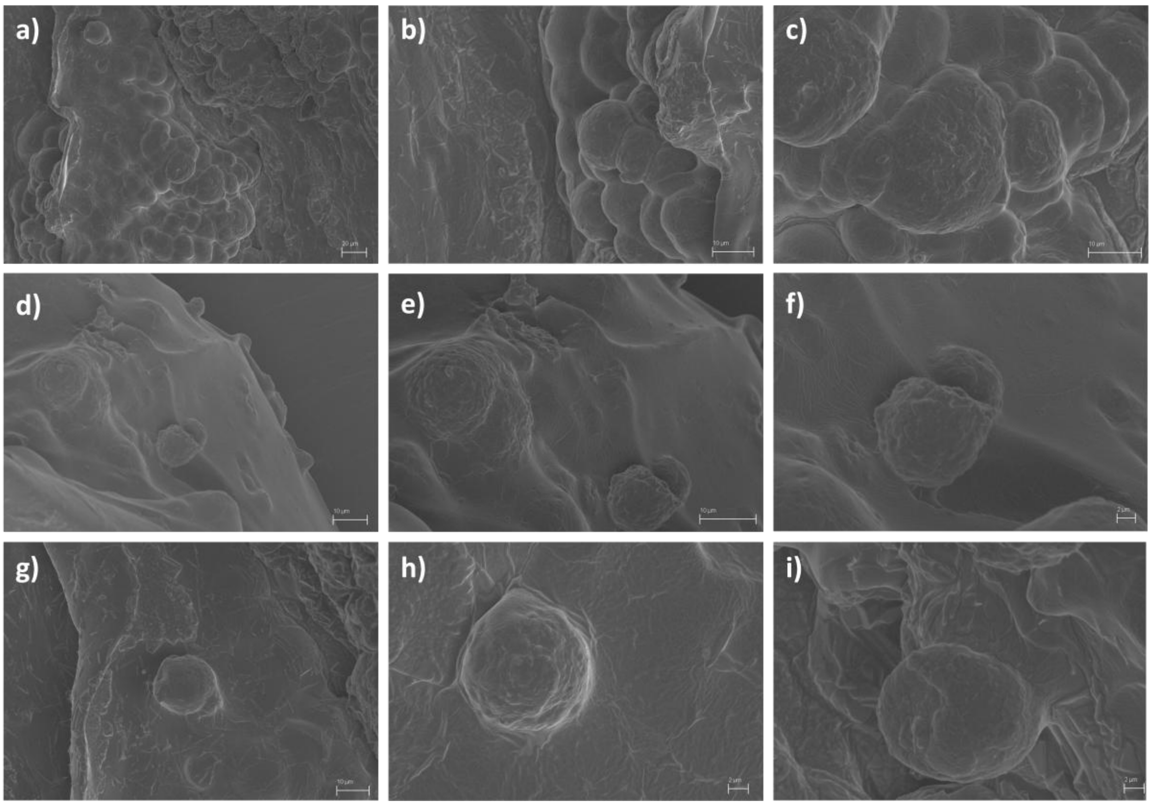

Figure 4-14. SEM images of EBs in 1.5%HA-3%PEGDA co-gels. SEM images of EBs formed in 1.5%HA-3%PEGDA hydrogels were obtained on Day 7 post-encapsulation.

4.3.3 Confocal microscopy

Confocal microscopy was done to capture images of EB formation in different planes of the hydrogel. Figure 4-15 again demonstrates EB formation in the hydrogel culture system. DAPI staining was also performed to prove the presence of nuclei in the EBs. A representative hydrogel sample, 1%HA-2%PEGDA, was utilized for imaging on Day 7. The tight mesh network of this hydrogel system inhibits EB growth and these EBs are not comparable in size to those found in 2D cultures. The positive DAPI does indicate multiple nuclei confirming the clustering of cells. Further imaging experiments can be done with less restrictive gels (i.e. pure HA hydrogels) to distinguish differences in EB size amongst hydrogel systems.

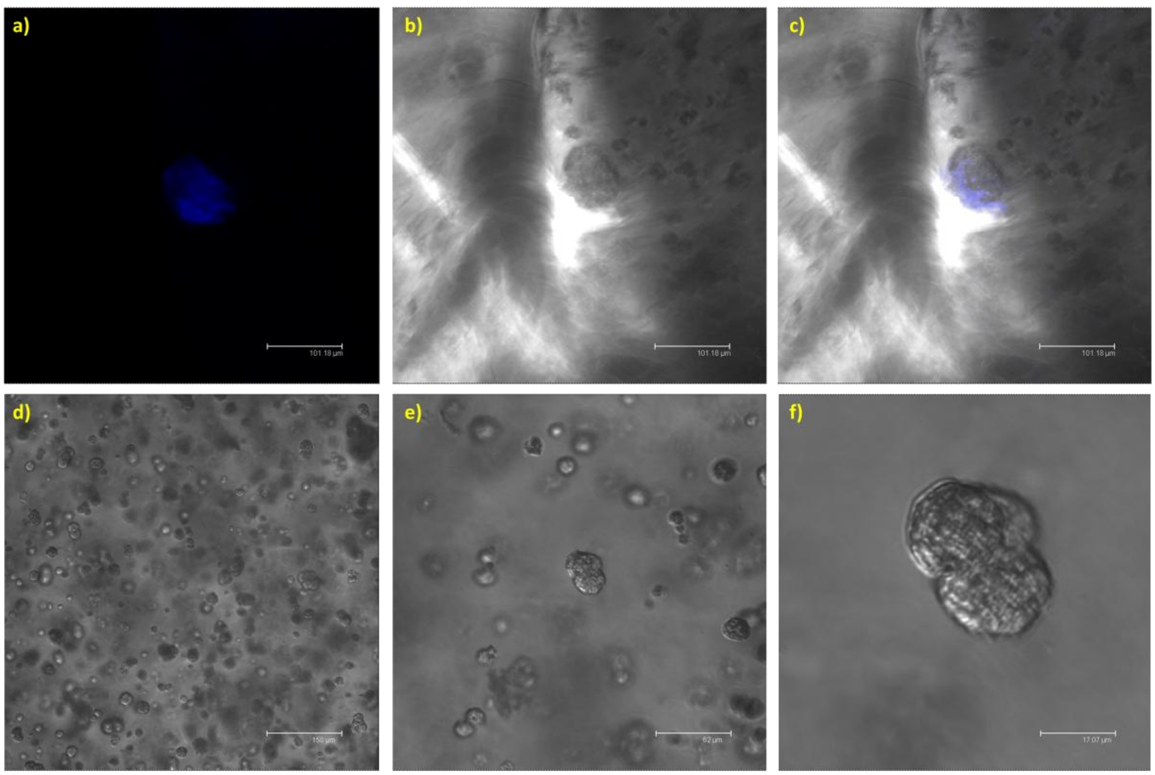

Figure 4-15. Confocal images of encapsulated mESCs. (a - c) Day 7 Encapsulated mESCs in 1%HA-2%PEGDA hydrogels were stained with DAPI to evaluate EB formation. (a) Confocal image of DAPI stain; (b) Normalsky image of EB associated with DAPI stain; (c) overlay of DAPI stain and Normalsky images obtained using LeicaLite Software. (d – f) Day 12 Normalsky images of encapsulated mESCs and EBs formed in 1.5%HA-3%PEGDA hydrogels.

4.4 mESC Differentiation

4.4.1 Flow cytometry

Cells from 2D control cultures and hydrogel cultures were fluorescently tagged with antibodies for cell surface markers c-kit and sca-1 and the intracellular marker, Oct-3/4, after 10 days in culture. The presence of Oct-3/4 in cells indicates stem cell maintenance. The existence of a double positive population (c-kit^{+}/sca-1^{+}) would designate hematopoietic differentiation in the culture. Samples were run through a flow cytometer and results were analyzed with the flow cytometry software, FlowJo. Figures 4-16 and 4-17 show the FACS results of two separate experiments with the exact same culture conditions. Both experiments were stopped on Day 10 and cell seeding density was constant. An unpaired, two-tailed student's t-test was used to determine statistically significant ($p < 0.05$) differences between hydrogel cultures and 2D controls in each experiment.

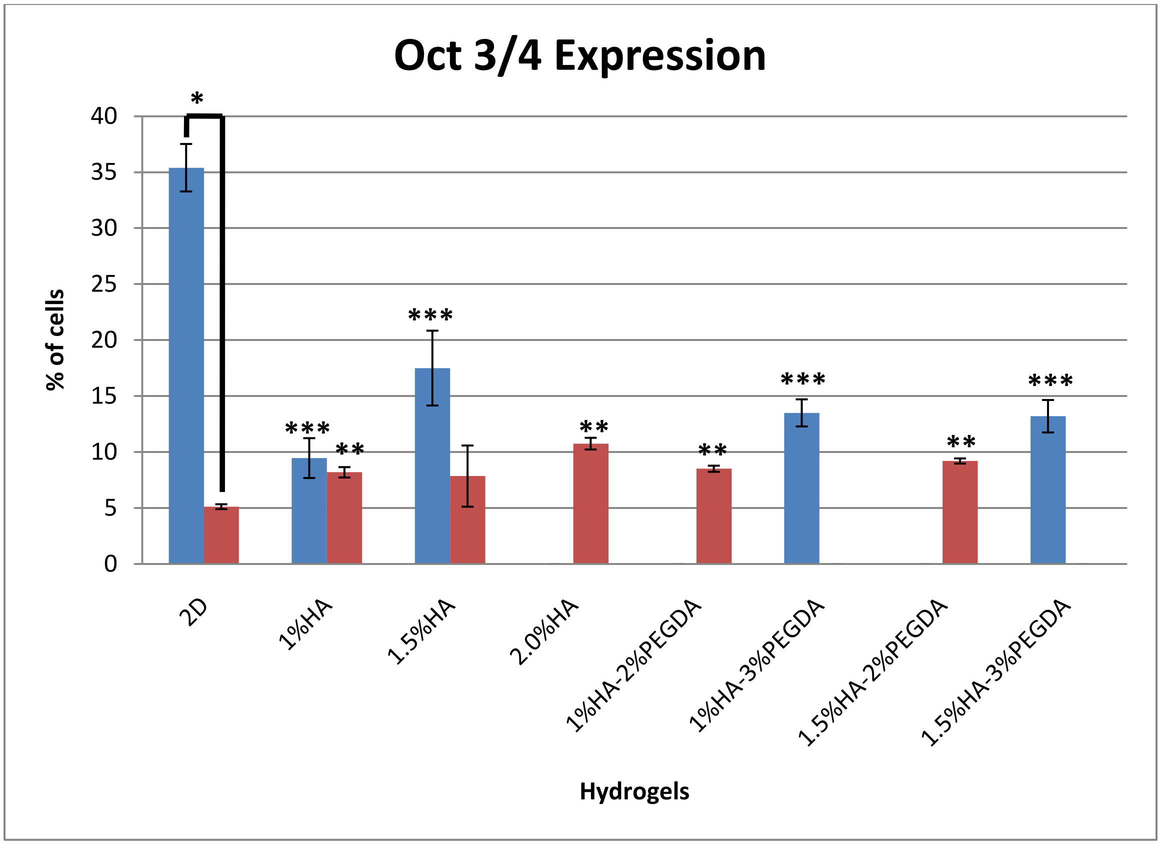

Figure 4-16. Expression of intracellular stem cell maintenance marker Oct-3/4 in 2D control and 3D hydrogel cultures. Flow cytometry analysis shows the level of expression in 2D control cultures and hydrogel systems. Blue bars and red bars are expression levels from two separate experiments, 1 and 2. (*) Oct-3/4 expression significantly different between experiments; (**) Oct-3/4 expression siginificantly different between hydrogel samples and 2D controls of experiment 1; (***) Oct-3/4 expression siginificantly different between hydrogel samples and 2D controls of experiment 2. Each data point is an average value ± standard error (n = 3).

A comparison of 2D control culture Oct-3/4 expression in both experiments reveals a drastic decline in percentage of Oct-3/4$^+$ cells. Results from the first experiment demonstrate a significant decrease in Oct-3/4$^+$ cells in hydrogel culture while results from the second experiment suggest an increase in Oct-3/4$^+$ in hydrogel culture compared to 2D cultures. The data from these experiments appears conflicting; however, the percentage of Oct-3/4^{+} cells in hydrogel cultures is consistently low. The percentage of Oct-3/4^{+} cells in all hydrogel samples ranges from only ~8% - 17% of the total cell population. Also, 1.0%HA and 1.5%HA hydrogels were examined in both experiments and there was no significant difference in total Oct-3/4^{+} cells in these cultures between experiments. Although the 2D culture Oct-3/4^{+} population varied greatly between experiments, the data illustrates small percentage of Oct-3/4^{+} cells in all culture conditions suggesting the occurrence of some form of differentiation in all culture systems.

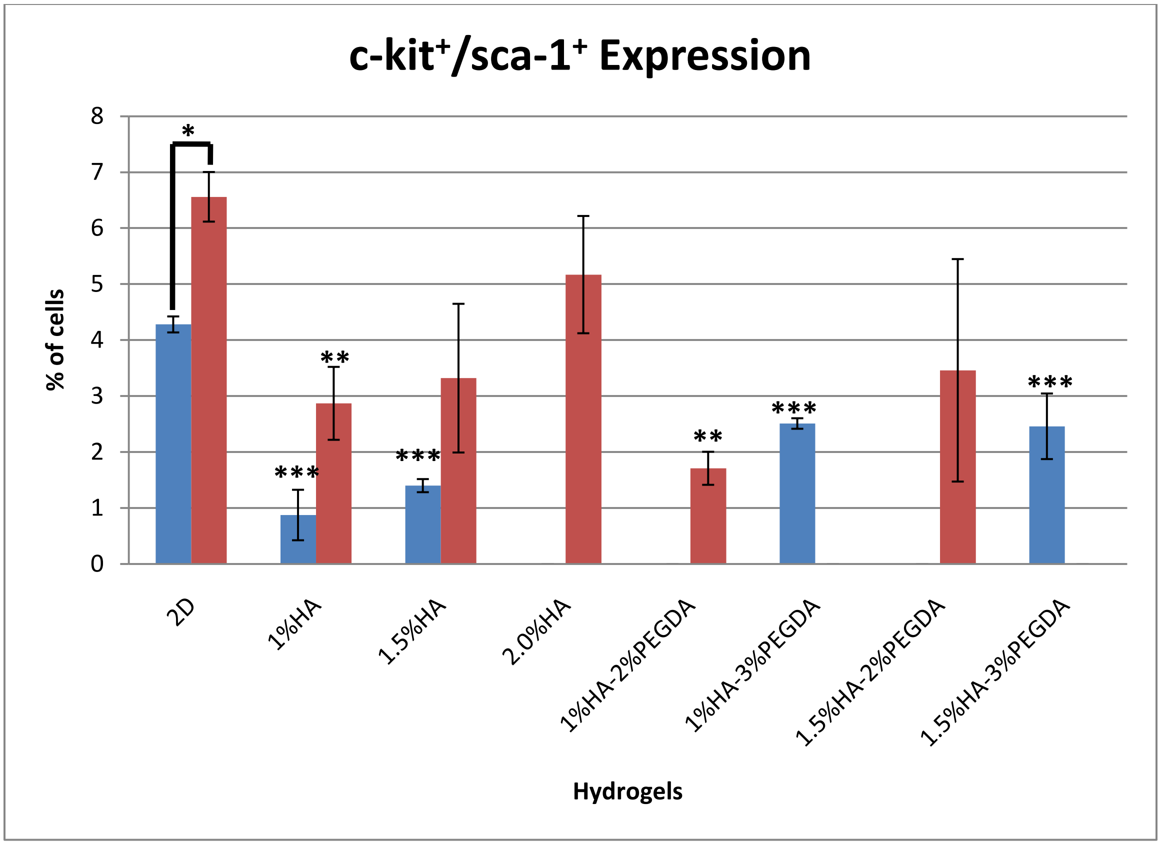

Figure 4-17. Expression of double positive cells for stem cell surface markers c-kit and sca-1 in 2D control and 3D hydrogel cultures. Flow cytometry analysis shows the level of expression in 2D control cultures and hydrogel systems. Blue bars and red bars are expression levels from two separate experiments, 1 and 2. (*) c-kit$^+$/sca-1$^+$ expression significantly different between experiments; (**)c-kit$^+$/sca-1$^+$ expression siginificantly different between hydrogel samples and 2D controls of experiment 1; (***) c-kit$^+$/sca-1$^+$ expression siginificantly different between hydrogel samples and 2D controls of experiment 2. Each data point is an average value ± standard error (n = 3).

In experiment 1 the c-kit$^+$/sca-1$^+$ double positive (DP) population in all hydrogel conditions used (1%HA, 1.5%HA, all 3% (w/v) co-gels) significantly decreased in comparison to 2D control cultures. The second experiment only showed a significant decrease in 1%HA and 1%HA-2%PEGDA hydrogel cultures. While the DP population for both 1.5%HA hydrogels and 1.5%HA-2%PEGDA co-gels in this experiment was not significant, the error on these sample are large compared to the means. Moreover, 1.5%HA hydrogel DP populations from the two experiments were not significantly different. This data suggests that the DP population decreases when mESCs are encapsulated but a decisive conclusion cannot be reached from this data and further repeats of this experiment must be conducted.

Figures 4-18 and 4-19 show the percentage of single positive c-kit and single positive sca-1 populations in the two experiments conducted. C-kit expression data from the two experiments is contradicting. In experiment 1, c-kit was shown to be significantly upregulated in the 3% (w/v) co-gel systems; experiment 2 demonstrated a significant decline in c-kit expression across all hydrogel systems with the exception of 2%HA.

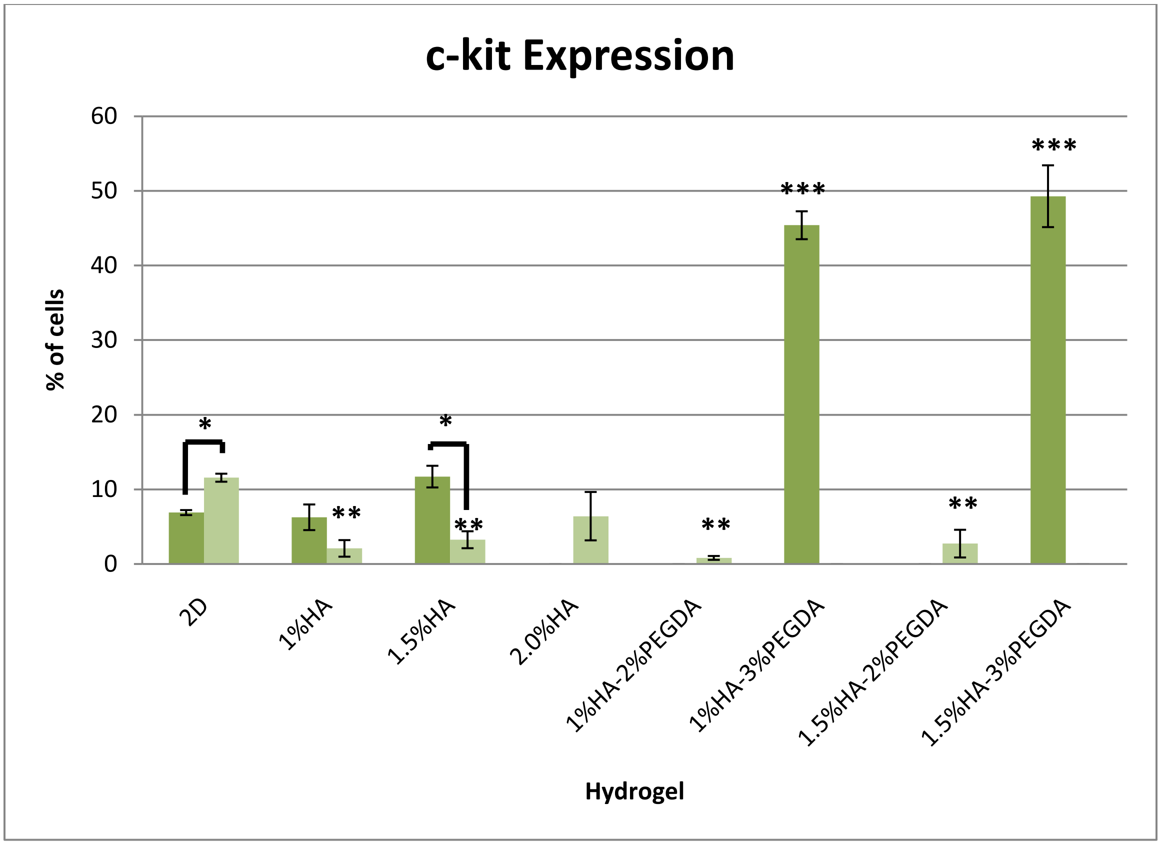

Figure 4-18. Expression of single positive cells for stem cell surface marker c-kit in 2D control and 3D hydrogel cultures. Flow cytometry analysis shows the level of c-kit expression in 2D control cultures and hydrogel systems. Blue bars and red bars are expression levels from two separate experiments, 1 and 2. (*) c-kit expression significantly different between experiments; (**) c-kit expression siginificantly different between hydrogel samples and 2D controls of experiment 1; (***) c-kit expression siginificantly different between hydrogel samples and 2D controls of experiment 2. Each data point is an average value ± standard error (n = 3).

In experiment 1, sca-1 expression dropped notably in the 3% (w/v) co-gel systems. Experiment 2, revealed a significant decrease in sca-1 expression only in 1.5%HA hydrogels. Both of the single positive data sets are inconclusive and a trend cannot be determined from cell marker expression analysis; therefore, expression of genes encoding for c-kit and sca-1 markers was conducted and will be discussed later in this thesis.

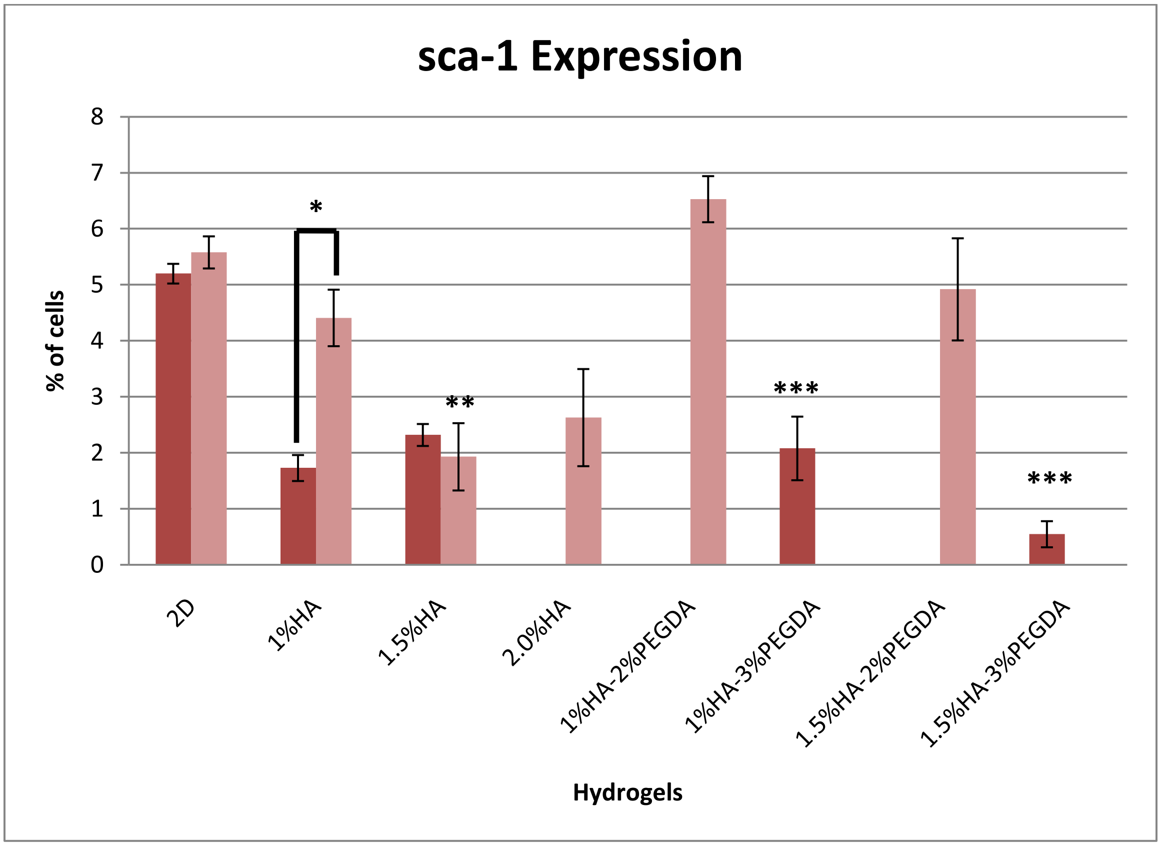

Figure 4-19. Expression of single positive cells for stem cell surface markers sca-1 in 2D control and 3D hydrogel cultures. Flow cytometry analysis shows the level of sca-1 expression in 2D control cultures and hydrogel systems. Blue bars and red bars are expression levels from two separate experiments, 1 and 2. (*) sca-1 expression significantly different between experiments; (**) sca-1 expression siginificantly different between hydrogel samples and 2D controls of experiment 1; (***) sca-1 expression siginificantly different between hydrogel samples and 2D controls of experiment 2. Each data point is an average value ± standard error (n = 3).

The presence of EBs evidenced through light microscopy, SEM, and confocal microscopy coupled with the Oct-3/4 data does suggest that differentiation is occurring in the hydrogels. However, the FACS data implies that the hydrogel culture systems are not as efficient at generating HSCs compared to 2D control cultures; the mESCs are not differentiating into the hematopoietic lineage. To attempt to determine the lineage which these cells are differentiating into a gene expression analysis was conducted.

4.4.2 PCR arrays

The RT^2 PCR Profiler Array for Embryonic Stem Cells was utilized to look at Day 7 up-regulation and down-regulation of genes associated with specific lineage markers as well as genes associated with stem cell maintenance, pluripotency, and self-renewal. Data was analyzed and statistical significance was determined using the Web-Based PCR Array Data Analysis software from SABiosciences. Included in the 84 genes on this array were primers Pou5f1 (the gene coding for Oct-3/4). Figure 4-20 illustrates the down-regulation of both this gene in hydrogel cultures compared to 2D control cultures. Although, none of these results were statistically significant ($p < 0.05$) the down-regulation of Pou5f1 corresponds with the FACS data showing decreased expression of Oct-3/4 indicating again that differentiation is occurring.

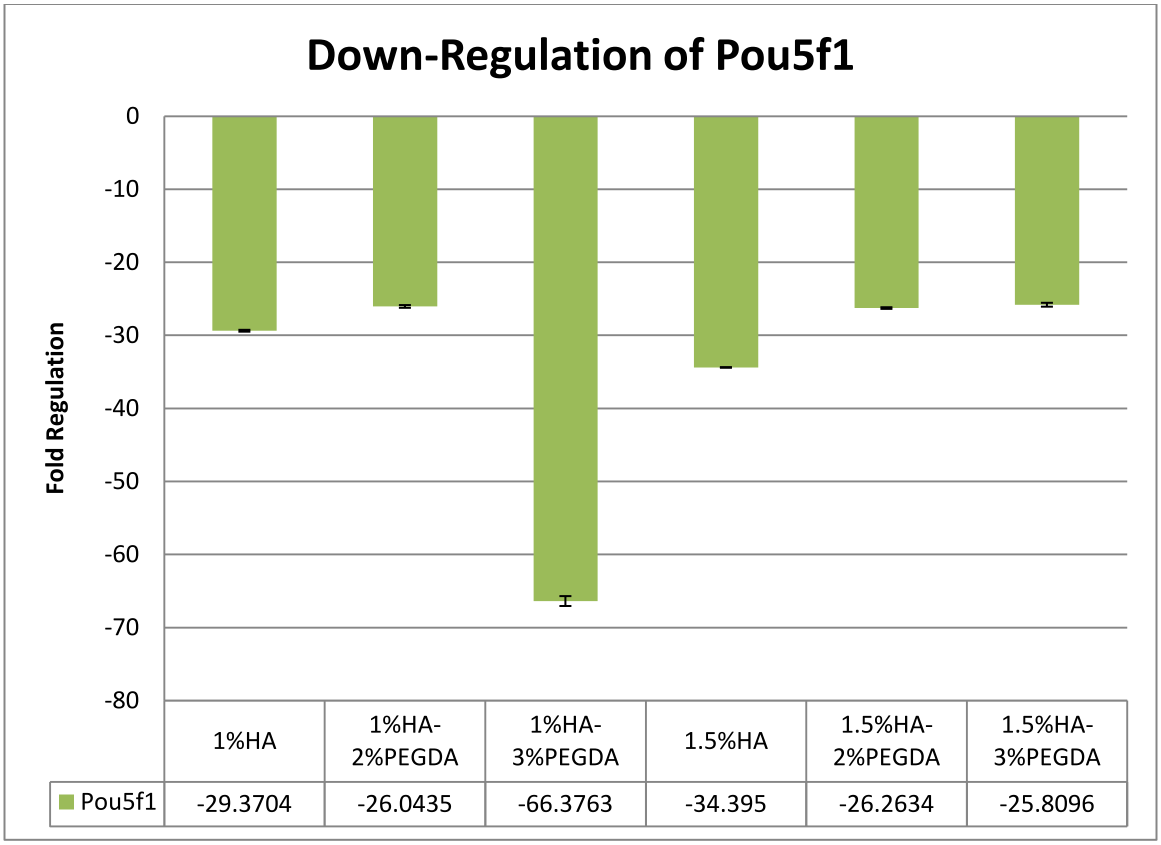

Figure 4-20. Down-Regulation of Pou5f1. RT-PCR array analysis of the Pouf51, the gene encoding for intracellular stem cell maintenance marker, Oct-3/4 shows gene expression of encapsulated cells in HA hydrogels and HA-PEGDA hydrogels in comparison to 2D control cultures. No gene expression values were found to be significantly different from 2D controls. Data was analyzed with SABiosciences web-based PCR Array data analysis software.

The only statistically significant data obtained from the 84 gene PCR array involved genes for blood lineage markers: Hemoglobin X, alpha-like embryonic chain in Hba complex (Hba-x) and Hemoglobin Y, beta-like embryonic chain (Hbb-y). Figure 4-21 displays the down-regulation of these two genes in hydrogels compared to 2D cultures.

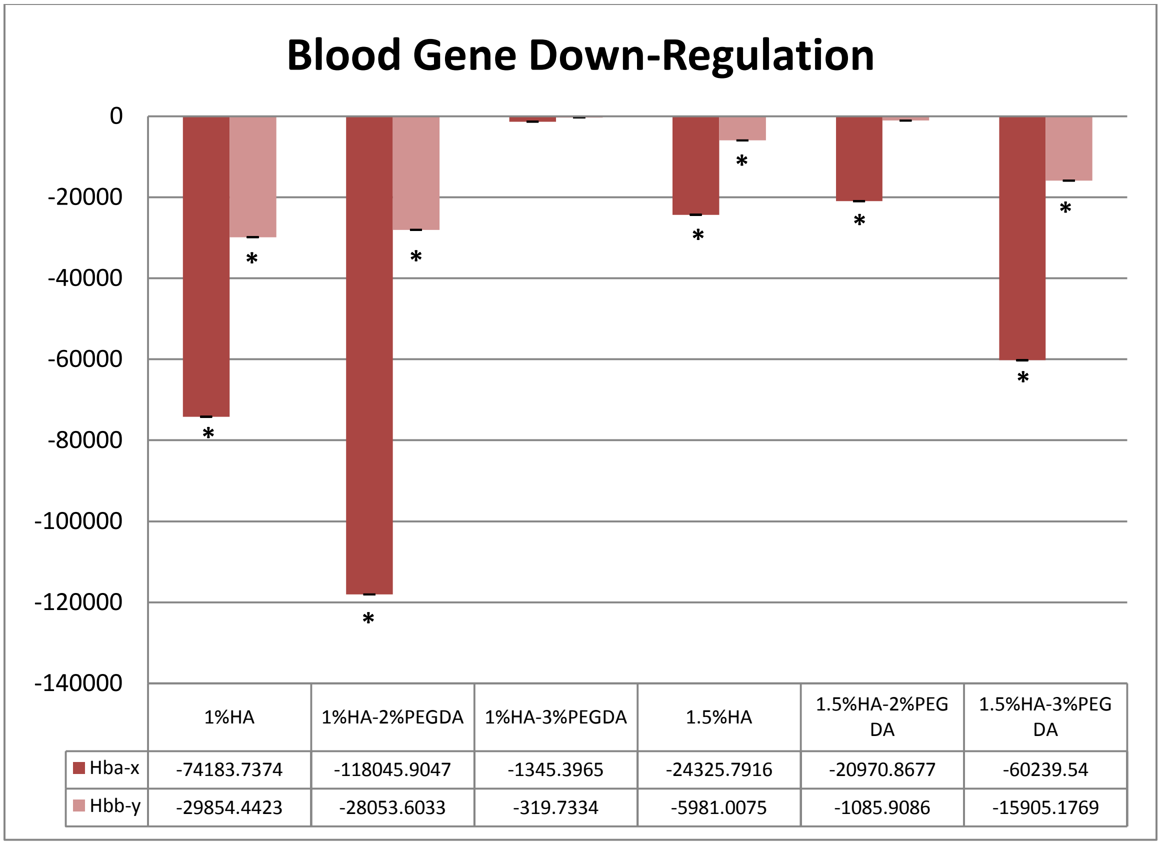

Figure 4-21. Down-Regulation of Blood Lineage Genes. RT-PCR array analysis of 84 genes shows down-regulation of Hba-x and Hba-y, genes associated with the blood lineage, in HA and HA-PEGDA hydrogel cultures in comparison to 2D control cultures. (*) Gene expression down-regulation statistically significant ($p < 0.05$) in comparison to 2D cultures. Data was analyzed with SABiosciences web-based PCR Array data analysis software.

4.4.3 Real-time polymerase chain reaction

RT-PCR was performed with primers for c-kit and sca-1; β-actin was used as a housekeeping gene. Fold change was calculated with the ΔΔCt method using the Ct values associated with 2D culture samples as control. Statistical significance ($p < 0.05$) was determined with a two-tailed, unpaired student's t-test. Figure 4-22 shows Day 7 gene fold change for c-kit and sca-1 in comparison to 2D culture gene expression levels.

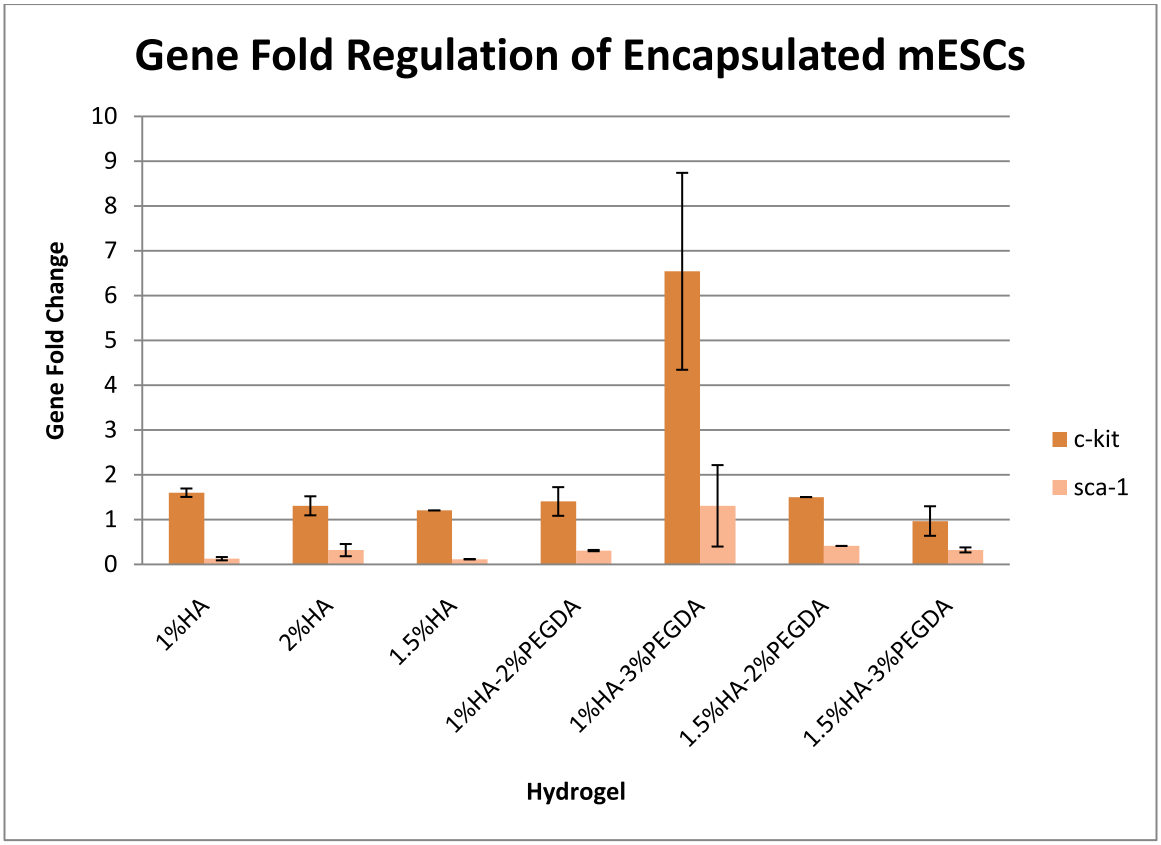

Figure 4-22. Gene Fold Regulation of Encapsulated mESCs. RT-PCR analysis genes encoding for stem cell markers, c-kit and sca-1, shows gene fold change in HA and HA-PEGDA hydrogel cultures in comparison to 2D control cultures. No gene fold changes were found to be significantly different. Each data point is an average value ± standard error (n = 3). Samples were run in triplicate. Data was analyzed using the ΔΔCt method.

The data reveals an up-regulation ranging from ~ 1-fold – 7-fold of the gene encoding for c-kit (Kit oncogene) across all hydrogel systems; however, KIT oncogene fold changes did not significantly differ across the hydrogel systems. The gene encoding for sca-1 (Ly6a) appears to not be up-regulated in the hydrogel systems with fold change values ranging from $\sim 0.1 - 1.3$. Up-regulation of only one of the hematopoietic markers is not sufficient to produce DP cells. These results are consistent with the DP FACS data revealing diminished DP cell populations in hydrogel systems. It is important to note that these gene expression trends are only slightly more conclusive than the preceding FACS data.

Chapter 5: Conclusion

A major hurdle to overcome in the field of regenerative medicine is the availability of a donor cell sources. Embryonic stem cells are capable of indefinite self-renewal and differentiation into any cell lineage making them an extremely attractive cell source in the field; however, driving the differentiation process to a specific lineage is a complicated process. Multiple factors may be responsible for lineage-specific differentiation including extrinsic physical and chemical factors, intrinsic cell signaling, cell-cell cross-communication, and receptor-ligand interactions. While a pluripotent cell source does essentially provide the researcher with a "blank slate" it also introduces another obstacle in lineage-specific differentiation: the potential of differentiation into multiple cell types, including or not including the lineage of interest. This thesis focused on elucidating the effects of a synthetic, biomimetic bone marrow microenvironment on mESC differentiation into the hematopoietic lineage.

The goal of this thesis was to produce a biocompatible hydrogel system which promotes hematopoietic differentiation of mESCs. Different variations of HA hydrogels and HA-PEGDA co-gels were formulated to develop microenvironments with varying pore sizes and degradation profiles in an attempt to determine the optimal hematopoietic 3D culture system. Although it was proven that these hydrogel systems provide a biocompatible microenvironment capable of maintaining a viable cell population with proliferative capacities, they are not efficient hematopoietic differentiation vehicles.

FACS data indicated a decreased expression of hematopoietic cell surface markers and RT-PCR revealed the up-regulation of Kit oncogene only. For effective hematopoietic differentiation, up-regulation of both Kit oncogene and Ly6a is necessary to express both hematopoietic cell surface markers, c-kit and sca-1. It appears that this system is not an effective hematopoietic differentiation cell culture system; however, data showing a decrease in Oct-3/4 expression and down-regulation of its gene, Pou5f1, as well as the formation of EBs in hydrogels suggests that differentiation is occurring in these 3D culture systems. PCR arrays were utilized in an attempt to identify which lineage encapsulated mESCs were being driven towards or if encapsulated mESCs were maintaining "stemness". The results obtained from the PCR array revealed that not only were none of the 84 genes markedly up-regulated but the only genes significantly down-regulated were those associated with the blood/hematopoietic lineage. Unfortunately, the PCR arrays did not provide any further information regarding lineage-specific differentiation of encapsulated mESCs. Additional cell marker and gene expression studies are necessary to confirm the results presented in this thesis.

Embryonic stem cells were cultivated in microenvironment similar to the native bone marrow, the anatomical site of hematopoeisis, but environmental cues presented to the cells were not sufficient to drive them towards the hematopoietic lineage. The hydrogels created may need further tailoring to be more akin to the native bone marrow. The bone marrow contains other proteins, GAGs, and supporting cells not included in this 3D culture system; it is possible that the incorporation of additional environmental factors may trigger hematopoietic differentiation. The introduction of chemical cues such as growth factors or placing the hydrogels in a dynamic or hypoxic environment may also help promote hematopoietic differentiation. The biocompatible HA-PEGDA hydrogel differentiation system created in this thesis can be used as a basis for future studies incorporating these other factors.

In conclusion, results presented in this thesis illustrate the complexities of ESCs and the difficulties in controlling lineage-specific differentiation. Advances in the regenerative medicine and tissue engineering fields may make ESCs the ideal cell source in future years; however, at the present time there are too many unknowns associated with ESCs. Extensive research must continue to be conducted in animal models before any significant societal impact can be made using embryonic stem cells.

References

[1] M. T. Mitjavila-Garcia, *et al.*, "Embryonic stem cells: Meeting the needs for cell therapy," *Advanced Drug Delivery Reviews,* vol. 57, pp. 1935-1943, Dec 2005.

[2] H. Liu, *et al.*, "Biomimetic three-dimensional cultures significantly increase hematopoietic differentiation efficacy of embryonic stem cells," *Tissue Engineering,* vol. 11, pp. 319-330, Jan 2005.

[3] S. Taqvi, *et al.*, "Influence of scaffold physical properties and stromal cell coculture on hematopoietic differentiation of mouse embryonic stem cells," *Biomaterials,* vol. 27, pp. 6024-6031, Dec 2006.

[4] S. Gerecht, *et al.*, "Hyaluronic acid hydrogen for controlled self-renewal and differentiation of human embryonic stem cells," *Proceedings of the National Academy of Sciences of the United States of America,* vol. 104, pp. 11298-11303, Jul 2007.

[5] A. L. Olsen, *et al.*, "Designer blood: creating hematopoietic lineages from embryonic stem cells," *Blood,* vol. 107, pp. 1265-1275, Feb 2006.

[6] J. A. Hackney, *et al.*, "A molecular profile of a hematopoietic stem cell niche," *Proceedings of the National Academy of Sciences of the United States of America,* vol. 99, pp. 13061-13066, Oct 2002.

[7] H. K. A. Mikkola and S. H. Orkin, "The journey of developing hematopoietic stem cells," *Development,* vol. 133, pp. 3733-3744, Oct 2006.

[8] L. S. Ferreira, *et al.*, "Bioactive hydrogel scaffolds for controllable vascular differentiation of human embryonic stem cells," *Biomaterials,* vol. 28, pp. 2706-2717, Jun 2007.

[9] S. M. Willerth, *et al.*, "Optimization of fibrin scaffolds for differentiation of murine embryonic stem cells into neural lineage cells," *Biomaterials,* vol. 27, pp. 5990-6003, Dec 2006.

[10] H. Liu, *et al.*, "Three-dimensional culture for expansion and differentiation of mouse embryonic stem cells," *Biomaterials,* vol. 27, pp. 6004-6014, Dec 2006.

[11] H. J. Rippon, *et al.*, "Derivation of distal lung epithelial progenitors from murine embryonic stem cells using a novel three-step differentiation protocol," *Stem Cells,* vol. 24, pp. 1389-1398, May 2006.

[12] M. Nakanishi, *et al.*, "Pancreatic tissue formation from murine embryonic stem cells in vitro," *Differentiation,* vol. 75, pp. 1-11, Jan 2007.

[13] Y. S. Hwang, *et al.*, "Enhanced derivation of osteogenic cells from murine embryonic stem cells after treatment with HepG2-conditioned medium and modulation of the embryoid body formation period: Application to skeletal tissue engineering," *Tissue Engineering,* vol. 12, pp. 1381-1392, Jun 2006.

[14] Z. J. Zhang, *et al.*, "Reorganization of actin filaments enhances chondrogenic differentiation of cells derived from murine embryonic stem cells," *Biochemical and Biophysical Research Communications,* vol. 348, pp. 421-427, Sep 2006.

[15] T. Yin, *et al.*, "The stem cell niches in bone," *Journal of Clinical Investigation,* vol. 116, pp. 1195-1201, May 2006.

[16] G. Lacaud, *et al.*, "Tracking mesoderm formation and specification to the hemangioblast in vitro," *Trends in Cardiovascular Medicine,* vol. 14, pp. 314-317, Nov 2004.

[17] J. Itskovitz-Eldor*, et al.*, "Differentiation of human embryonic stem cells into embryoid bodies comprising the three embryonic germ layers," *Molecular Medicine,* vol. 6, pp. 88-95, Feb 2000.

[18] N. D. Evans*, et al.*, "Scaffolds for stem cells," *Materials Today,* vol. 9, pp. 26-33, Dec 2006.

[19] S. M. Dang*, et al.*, "Efficiency of embryoid body formation and hematopoietic development from embryonic stem cells in different culture systems," *Biotechnology and Bioengineering,* vol. 78, pp. 442-453, May 2002.

[20] A. Wilson*, et al.*, "Bone-marrow haematopoietic-stem-cell niches," *Nature Reviews Immunology,* vol. 6, pp. 93-106, Feb 2006.

[21] D. N. Haylock*, et al.*, "Stem cell regulation by the hematopoietic stem cell niche," *Cell Cycle,* vol. 4, pp. 1353-1355, Oct 2005.

[22] S. K. Nilsson*, et al.*, "Hyaluronan is synthesized by primitive hemopoietic cells, participates in their lodgment at the endosteum following transplantation, and is involved in the regulation of their proliferation and differentiation in vitro," *Blood,* vol. 101, pp. 856-862, Feb 2003.

[23] N. S. Hwang*, et al.*, "Enhanced chondrogenic differentiation of murine embryonic stem cells in hydrogels with glucosamine," *Biomaterials,* vol. 27, pp. 6015-6023, Dec 2006.

[24] N. S. Hwang*, et al.*, "Response of zonal chondrocytes to extracellular matrix-hydrogels," *Febs Letters,* vol. 581, pp. 4172-4178, Sep 2007.

[25] S. K. Nilsson*, et al.*, "Immunofluorescence characterization of key extracellular matrix proteins in murine bone marrow in situ," *Journal of Histochemistry & Cytochemistry,* vol. 46, pp. 371-377, Mar 1998.

[26] T. N. Wight*, et al.*, "PROTEOGLYCANS IN HUMAN LONG-TERM BONE-MARROW CULTURES - BIOCHEMICAL AND ULTRASTRUCTURAL ANALYSES," *Blood,* vol. 67, pp. 1333-1343, May 1986.

[27] D. N. Haylock and S. K. Nilsson, "The role of hyaluronic acid in hemopoietic stem cell biology," *Regenerative Medicine,* vol. 1, pp. 437-445, Jul 2006.

[28] M. I. Tammi*, et al.*, "Hyaluronan and homeostasis: A balancing act," *Journal of Biological Chemistry,* vol. 277, pp. 4581-4584, Feb 2002.

[29] T. C. Laurent and J. R. E. Fraser, "HYALURONAN," *Faseb Journal,* vol. 6, pp. 2397-2404, Apr 1992.

[30] J. E. Scott*, et al.*, "SECONDARY AND TERTIARY STRUCTURES OF HYALURONAN IN AQUEOUS-SOLUTION, INVESTIGATED BY ROTARY SHADOWING ELECTRON-MICROSCOPY AND COMPUTER-SIMULATION - HYALURONAN IS A VERY EFFICIENT NETWORK-FORMING POLYMER," *Biochemical Journal,* vol. 274, pp. 699-705, Mar 1991.

[31] P. Prehm, "IDENTIFICATION AND REGULATION OF THE EUKARYOTIC HYALURONATE SYNTHASE," *Ciba Foundation Symposia,* vol. 143, pp. 21-40, 1989.

[32] L. M. Pilarski*, et al.*, "REGULATED EXPRESSION OF A RECEPTOR FOR HYALURONAN-MEDIATED MOTILITY ON HUMAN THYMOCYTES AND T-CELLS," *Journal of Immunology,* vol. 150, pp. 4292-4302, May 1993.

[33] L. M. Pilarski*, et al.*, "RHAMM, A RECEPTOR FOR HYALURONAN-MEDIATED MOTILITY, ON NORMAL HUMAN-LYMPHOCYTES, THYMOCYTES AND MALIGNANT B-CELLS - A MEDIATOR IN B-CELL MALIGNANCY," *Leukemia & Lymphoma,* vol. 14, pp. 363-374, Aug 1994.

[34] E. A. Turley*, et al.*, "EXPRESSION AND FUNCTION OF A RECEPTOR FOR HYALURONAN-MEDIATED MOTILITY ON NORMAL AND MALIGNANT LYMPHOCYTES-B," *Blood,* vol. 81, pp. 446-453, Jan 1993.

[35] S. L. Gares*, et al.*, "During human thymic development, beta(1) integrins regulate adhesion, motility, and the outcome of RHAMM/hyaluronan engagement," *Journal of Leukocyte Biology,* vol. 64, pp. 781-790, Dec 1998.

[36] A. Avigdor*, et al.*, "CD44 and hyaluronic acid cooperate with SDF-1 in the trafficking of human CD34(+) stem/progenitor cells to bone marrow," *Blood,* vol. 103, pp. 2981-2989, Apr 2004.

[37] J. B. Leach*, et al.*, "Photocrosslinked hyaluronic acid hydrogels: Natural, biodegradable tissue engineering scaffolds," *Biotechnology and Bioengineering,* vol. 82, pp. 578-589, Jun 2003.

[38] J. B. Leach*, et al.*, "Photocrosslinked hyaluronic acid hydrogels: Natural, biodegradable tissue engineering scaffolds," *Biotechnology and Bioengineering,* vol. 82, pp. 578-589, Jun 2003.

[39] H. P. Tan*, et al.*, "Injectable in situ forming biodegradable chitosan-hyaluronic acid based hydrogels for cartilage tissue engineering," *Biomaterials,* vol. 30, pp. 2499-2506, May 2009.

[40] J. A. Wieland*, et al.*, "Non-viral vector delivery from PEG-hyaluronic acid hydrogels," *Journal of Controlled Release,* vol. 120, pp. 233-241, Jul 2007.

[41] R. L. Williams*, et al.*, "MYELOID-LEUKEMIA INHIBITORY FACTOR MAINTAINS THE DEVELOPMENTAL POTENTIAL OF EMBRYONIC STEM-CELLS," *Nature,* vol. 336, pp. 684-687, Dec 1988.

Vita

Kathryn Marie Erickson was born on May 25, 1984 in Plainfield, New Jersey to Carolyn Marie Erickson and Edward Emil Erickson. Kathryn grew up in Warren Township, New Jersey and graduated from Watchung Hills Regional High School in 2002. She attended Boston College in Chestnut Hill, Massachusetts where she received her Bachelor of Science in Biology in 2006. She then moved to Austin, Texas in August 2006 to pursue graduate studies in Biomedical Engineering at the University of Texas at Austin. She worked as a graduate research assistant for three years in the Laboratory for Cellular and Macromolecular Engineering under the supervision of Dr. Krishnendu Roy.

Permanent Address: 8515 Brodie Lane, Apartment 1016
Austin, TX 78745

This thesis was typed by Kathryn Marie Erickson.